

# **Fabrication, Structural characterization and Impedance analysis of Erbium(Er) & Copper (Cu) co-doped Zinc Oxide (ZnO)**



**Khair Un Nisa**  
**Fall 2017-MS Physics**  
**Regn. # 00000203347**




A thesis submitted in partial fulfillment of the requirements  
For the degree of **Master of Science**  
in  
**Physics**

**Supervised By: Dr Fahad Azad**

Department of Physics  
School of Natural Sciences (SNS)  
National University of Sciences and Technology (NUST)  
H-12, Islamabad, Pakistan 2017-2019

**National University of Sciences & Technology****MS THESIS WORK**

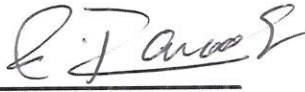
We hereby recommend that the dissertation prepared under our supervision by: Ms. Khair un Nisa, Regn No. 00000203347 Titled: **Fabrication, Structural characterization and Impedance analysis of Erbium(Er) & Copper (Cu) co-doped Zinc Oxide (ZnO)** accepted in partial fulfillment of the requirements for the award of MS degree.

**Examination Committee Members**1. Name: DR. FAHEEM AMINSignature: 2. Name: DR. RIZWAN KHALIDSignature: External Examiner: DR. ZULQARNAIN ALISignature: Supervisor's Name DR. FAHAD AZADSignature: 

  
Head of Department

28/12/2020  
Date

**COUNTERSIGNED**Date: 28-12-2020

  
Dean/Principal


## THESIS ACCEPTANCE CERTIFICATE

Certified that final copy of MS thesis written by Ms. Khair un Nisa (Registration No. 00000203347), of School of Natural Sciences has been vetted by undersigned, found complete in all respects as per NUST statutes/regulations, is free of plagiarism, errors, and mistakes and is accepted as partial fulfillment for award of MS/M.Phil degree. It is further certified that necessary amendments as pointed out by GEC members and external examiner of the scholar have also been incorporated in the said thesis.


Signature: 

Name of Supervisor: Dr. Fahad Azad

Date: 28-12-2020

Signature (HoD): 

Date: 28/12/2020

Signature (Dean/Principal): 

Date: 28-12-2020

*Dedicated to my Parents,  
Brother, Grandmother  
and my late Uncle (RIP)*

## **Acknowledgements**

Thanks to Allah Almighty for giving me courage to complete my MS degree. During my research, there were a lot of people whose support and insight have proved indispensable. In particular, I owe my deepest gratitude to my Supervisor **Dr Fahad Azad** for all his help, advice and teaching. His eagerness and unlimited avidity has been the major driving force for me to do the quality work. He has always been kind, supportive and above all critical about the work. I would also like to thank my guidance committee members Dr. Fahim Ameen and Dr. Rizwan Khalid. Their productive criticism helped me in improvising my work.

My class fellows and friends have been a continuous source of support, especially Ayesha Zaheer, Zaheer Ud din Babar, Fatima Shahid, Danish Ali Hamza ,Zeeshan Rashid, Huma Tariq and Saira Parveen. Last but not least I pay my deepest gratitude to my Mother and Father for putting their confidence in me and trusting me even at my lowest. I owe them a lot.

*Khair Un Nisa*

# Abstract

Materials which have the value of real part of dielectric constant  $\epsilon' > 10^3$  are known as Colossal dielectric constant materials. They have vast applications in microelectronics, compact and high energy storage devices. This research work is employed to use Zinc Oxide as Colossal dielectric constant material. To tailor its dielectric properties the material is co doped with Erbium and copper, Erbium acts as a donor and copper as an acceptor in ZnO. From XRD results it has been proved that both Erbium and copper are successfully doped in ZnO with 0.25, 0.5, 0.75 and 1%M doping concentrations. Band gap analysis of all the samples is done using UV visible Diffuse Reflectance Spectroscopy. After a successful insight about the substitutional doping in ZnO through XRD, the samples are analyzed through Impedance spectroscopy. Impedance analysis of the samples confirmed the colossal permittivity in ZnO which increases with an increase in doping concentration. 1% co-doped ZnO sample has a maximum value of dielectric constant. It is observed that the value of real part of dielectric constant decreased with an increase in frequency while ac conductivity increased with an increase in frequency.

# Contents

<b>Chapter 1: Introduction</b> .....	<b>8</b>
1.1) Motivation and Objective: .....	8
1.2) Zinc Oxide (ZnO) – An Introduction: .....	10
1.2.1) Crystal structure of ZnO: .....	10
1.3) Applications of ZnO in Industry: .....	12
1.4) Fundamentals of ZnO as a semiconductor: .....	13
1.4.1) Advantages of ZnO over GaN: .....	14
1.4.2) Bandgap engineering of ZnO: .....	14
1.5) Doping and defect chemistry in ZnO: .....	15
1.5.1) Intrinsic Defects: .....	15
1.5.2) Doping in ZnO: .....	17
1.5.2.1) Acceptor Impurities: .....	17
1.5.1.2) Donor Impurities: .....	18
1.6) Role of interstitial and substitutional H in n-type conductivity: .....	19
<i>Scaling of the devices:</i> .....	20
1.7) Introduction to dielectric material .....	20
1.7.1) Dielectric constant: .....	22
1.7.2) Dielectric Polarization: .....	23
<b>Chapter 2: Synthesis and Literature Review</b> .....	<b>25</b>
2.1) Synthesis Method: .....	25
2.1.1) Sol-Gel: .....	25
Detail of the process: .....	25
2.2) Synthesis of undoped and Er, Cu- doped ZnO: .....	27
2.2.1) Undoped ZnO: .....	29
Procedure .....	29
2.2.2) co-doped ZnO: .....	29
Procedure: .....	30
2.2 Literature Review and Background: .....	31
<b>Chapter 3: Characterization Techniques</b> .....	<b>34</b>
3.1.1) Fundamental Principle of X-ray Powder Diffraction: .....	35
Bragg's Law: .....	35
3.2) Diffuse Reflectance Spectroscopy (DRS): .....	36

3.2.2) Diffuse Interreflection: .....	39
3.3) Impedance Spectroscopy (IS):.....	41
3.3.1) Working principle of impedance:.....	41
Nyquist Plot: .....	45
Bode Plot: .....	46
3.3.2) Elementary Analysis Of Impedance Spectra .....	47
3.3.2.1) IS Plots of some model systems:.....	47
Ionic solid with two blocking electrodes: .....	47
<b>Chapter 4: Results and discussions.....</b>	<b>50</b>
4.1) X-Ray Diffraction: .....	50
4.1.1) Calculation of crystallite size and Micro Strain from XRD data using Williamson-Hall (W-H) Plot: .....	52
4.2) Band Gap Calculation using Kubelka-Munk Treatment: .....	57
4.3) Impedance Analysis: .....	60
4.3.1) Impedance plan plot ( $Z''$ Vs $Z'$ ):.....	60
4.3.2) Frequency Vs Dielectric Constant: .....	62
4.3.3) Frequency Vs Tangent losses: .....	63



# List of Figures:

Fig 1. 1 Unit cell of ZnO, small gray and larger red circles represent Zn and O atoms, respectively.....	10
Fig 1. 2 Types of defects that may occur in ZnO.....	15
Fig 1. 3 a) Formation energy of defects in ZnO in Oxygen rich and poor environment b) relative fermi energy .....	16
Fig 1. 4 This shows Coupling among H 1s orbital and Zn 4s dangling bonds (Zn dbs) to make the H multicenter bond in ZnO.....	19
Fig 1. 5 A polarized dielectric material (parallel plate capacitor).....	20
Fig 2. 1 Illustration of Sol gel method.....	26
Fig 2. 2 A visual representation of the process of synthesis .....	28
Fig 3. 1 Advance D8 XRD machine .....	35
Fig 3. 2 Illustration of Bragg's Law .....	36
Fig 3. 3 UV-Visible Diffuse Reflectance Spectrophotometer .....	37
Fig 3. 4 It is a depiction of diffuse and specular reflection from an absurd and glossy surface respectively.....	37
Fig 3. 5 Diffuse Reflection through a solid .....	38
Fig 3. 6 Interactions at grains and grain boundaries.....	41
Fig 3. 7 Illustration of the setup for IS .....	43
Fig 3. 8 Nyquist Plot; Fig3. 9 Nyquist plot as a function of frequency .....	45
Fig 3. 10 A typical Bode Plot .....	46
Fig 3. 11 Equivalent circuit .....	48
Fig 3. 12 Impedance plot for the equivalent circuit .....	48
Fig 3. 13 Experimental results of the given example .....	49
Fig 4. 1 XRD pattern of un doped and co-doped samples of ZnO.....	51
Fig 4. 2 W-H Plot of un-doped ZnO .....	55
Fig 4. 3 W-H Plots of 0.25, 0.5, 0.75 and 1% co-doped ZnO.....	55
Fig 4. 4 Diffuse Reflectance spectra (Band Gap energies) i.e Munk plot of undoped ZnO.....	57
Fig 4. 5 Munk plot of 0.25% Er,Cu doped ZnO .....	58
Fig4. 6 Munk plot of 0.5% Er,Cu doped ZnO .....	58
Fig 4. 7 Munk plot of 0.75% Er,Cu doped ZnO .....	59
Fig 4. 8 Munk plot of 1% Er,Cu doped ZnO .....	59
Fig 4. 9 Nyquist plots of 0.5 0.75 and 1% co-doped ZnO .....	61
Fig 4. 10 Variation of real part of the dielectric constant w.r.t frequency for 0.5, 0.75 and 1% co-doped ZnO annealed.....	63
Fig 4. 11 Variation of tangent loss w.r.t frequency for 0.5,0.75 and 1% co-doped ZnO .....	64

# Chapter 1: Introduction

---

## 1.1) Motivation and Objective:

Colossal dielectric permittivity (CP) materials have gained rigorous contemplation due to their prospective applications in microelectronics and energy storage devices. Substantial research has been executed on ferroelectric materials and non-ferroelectrics like  $\text{CaCu}_3\text{Ti}_4\text{O}_{12}$  [22-26] to get high permittivity. At the same time, the dependence of permittivity on temperature and frequency has confined their use in device miniaturization. For the accomplishment of CP material, the host material must fulfill some of the following phenomena such as ferroelectricity, hopping charge transport, surface barrier layer capacitance (SBLC), or metal-insulator transition. In ceramics, CP is ascribed to the internal barrier layer capacitance effect (IBLC)[27,28]. Most recently a defect engineering approach is employed for the achievement of colossal dielectric permittivity in metal oxides. The localization of carriers i.e electrons or holes into substitutional defects are found to be the main reason for CP in these materials. A very low dielectric loss has been observed in these materials due to hopping of localized defects. Temperature and frequency independent CP and dielectric loss have been observed recently in In, Nb co-doped  $\text{TiO}_2$ . The formation of local delocalized electrons resulting in electron-pinned defect-dipoles due to incorporation of the donor (Nb) and acceptor (In) impurity at the same time in  $\text{TiO}_2$  is the reason for observed CP.

Extensive research work has been done to achieve high dielectric constant in ferroelectric materials, but still, there is no successful accomplishment in achieving temperature and frequency independent ferroelectrics. Temperature independent dielectric constant was observed in non-ferroelectric materials but they exhibit very high tangent losses. Therefore, compendious research work is required to fabricate materials that show temperature and frequency independent CP and minimum dielectric losses. This research work aims to employ **Zinc Oxide (ZnO)** for the realization of CP by using a defect

engineering approach in which electrons can be localized in substitutional defects or amorphous structure.

The majority of the research on ZnO has been executed to understand unintentional n-type conductivity due to its native defects. It is reported that Mg-doped ZnO behaves as a promising CP material with colossal dielectric permittivity up to  $10^4$  due to the IBLC mechanism [29]. The basic aim of this research work is to employ ZnO to achieve temperature and frequency independent colossal permittivity in this material, although it has already been reported that ZnO has CP behavior but its dependence on frequency and temperature has restricted its use in high storage energy devices. So, it is need of the hour to discover a way in which materials show a high dielectric permittivity independent of temperature and frequency. In this project the effect of co-doping on ZnO will be seen, ZnO will be doped with acceptor as well as donor impurities at the same time. Copper will be used as an acceptor whereas Erbium will act as a donor impurity. As it is well known that native point defects play an important role in determining dielectric properties, therefore, it is obligatory to understand the complete story of defect mechanism and its correlation with dielectric properties. In this work, we intend to interpret the physics behind CP of ZnO by the recruitment of unique experimental techniques. This approach will open up new ways for the researchers to use ZnO for the comprehension of ZnO as a CP material with minimum dielectric losses. Let's begin with the brief introduction (i.e structural and other properties) of ZnO, which is accompanied in the following section.

## 1.2) Zinc Oxide (ZnO) - An Introduction:

### 1.2.1) Crystal structure of ZnO:

At the circumjacent environment, ZnO possesses a wurtzite crystalline structure. It has a hexagonal unit cell. It is clearly shown in Fig 1.1 that the crystal structure of ZnO is fashioned of two pervading hexagonal closed pack (hcp) sublattices. In which atoms are displaced concerning others through the threefold axis. It has  $sp^3$  covalent bonding in which at the section of the tetrahedron every anion is circumscribed by four cations in hexagonal ZnO. In Addition to the wurtzite phase, ZnO is believed to exist in cubic zincblende and rocksalt structures. Zinc blende ZnO and rock salt structures of ZnO are different from each other in such a way that zinc blende is only stable when grown on cubic structures while rock salt structure can't be stabilized epitaxially. At very high temperatures ZnO can exist in other phases like cesium chloride.

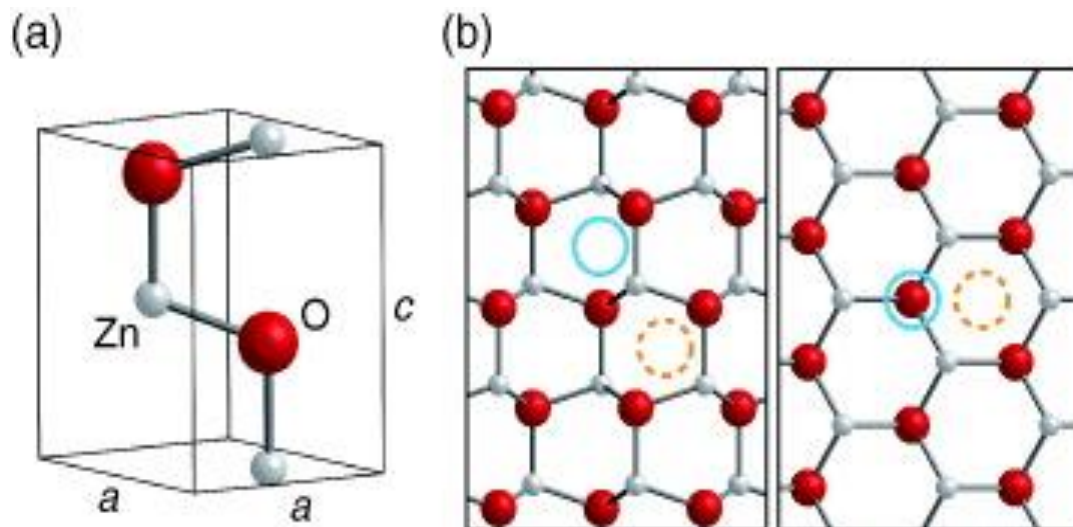
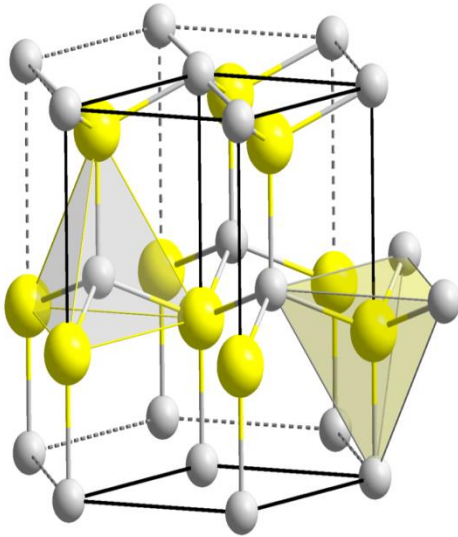


Fig 1. 1: Unit cell of ZnO, small gray and larger red circles represent Zn and O atoms, respectively.

### a) Wurtzite structure



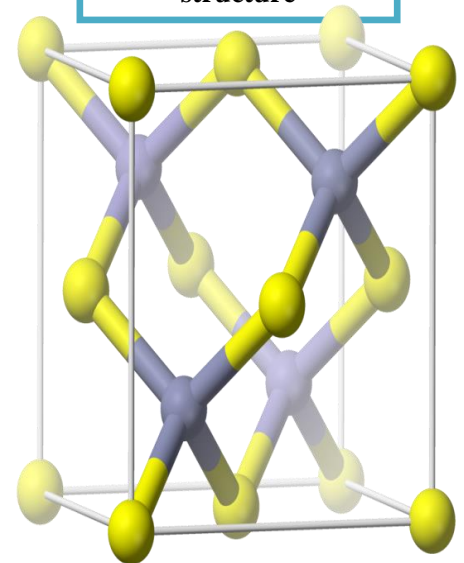
ZnO is a comparatively soft material [1]. In a competition to other semiconductors of the same group, it has smaller elastic constants. Due to its high melting temperature, it is very beneficial in Ceramics[2]. It has a very high piezoelectric tensor which makes it complementary to be used for piezoelectric Applications [3]. There are many advantages linked with ZnO due to its large bandgap i.e 3.3eV at room temperature. This larger bandgap gives ZnO the strength to endure large electric fields which results in lesser noise. By amalgamating with MgO or CdO can be tuned even up to 3.4eV [4]. Paradoxically, in the

absence of interstitial doping ZnO exhibits n-type character. The origin of the n-type behavior of ZnO is generally related to non-stoichiometry, but it remains controversial that what is the actual explanation for that? [5]. Another explanation was given i.e substitutional hydrogen impurities are the cause of unintentional n-type behavior [6].

Although ZnO exhibits n-type behavior this character can be further tuned by substituting Zn with group III elements such as Ga or substituting oxygen with group VII elements like Cl [7]. ZnO does not show p-type behavior intentionally, it remains hard to obtain p-type character. This limitation of achieving p-type doping somehow limits the applications of ZnO in Optoelectronics because there you need junctions of n-type and p-type material. One of the famous p-type dopants is group I elements; group V elements, as well as Cu and Ag. Most of these dopants form a deep acceptor level, so they do not give noteworthy p-type conduction at room temperature [4].

Near UV and visible regions ZnO exhibits high optical transparency and remarkable luminescent properties [8]. Due to these properties, ZnO is a propitious material for optoelectronic applications such as in gas sensors, solar cells and surface acoustic devices, etc [9]. ZnO has a high exciton binding energy that is

### b) Cubic Zinc blend structure



approximately 60meV which allows excitonic emissions even at room temperature, which makes it achieve high radiative recombination efficiency for spontaneous emission and lower threshold voltage for laser emission. There are many studies going on to improve the properties of ZnO to adapt it for various applications; for instance, the bandgap of ZnO is adjusted such that it can be used as UV detectors. ZnO nanoparticles are deployed in many potential applications and rudimentary research, such as field emitters, ultraviolet lasers and diodes, photocatalysts and piezoelectric devices [10], controlling units as UV photodetectors and as high flame detectors [11,12].

### **1.3) Applications of ZnO in Industry:**

There are plenty of applications of ZnO powder, the principal ones are described below. ZnO has high thermal conductivity, high refractive index, antibacterial, and UV protection properties for material science applications.

- ZnO is utilized in the rubber industry up to 50 to 60% of its total usage [13]. It is utilized in the vulcanisation of rubber. ZnO additives are used as protection from UV light and fungi. A substantial amount of ZnO is consumed by the ceramic industry, particularly in the ceramic glaze (in metallurgy). The relatively high heat capacity and high-temperature stability make ZnO desirable to be used in ceramics. ZnO helps to avert shuddering of ceramics due to improved elasticity of glazes.
- A consequential amount of ZnO is used in the medicine industry. A mixture of ZnO consisting of 0.5%  $\text{Fe}_2\text{O}_3$  is called calamine and is utilized for making a lotion. ZnO when mixed with a ligand and eugenol forms ZnO eugenol, which has huge applications in dentistry [14]. The fine particles of ZnO have sanitizing as well as antibacterial properties, due to which they are added into the oral care products. Zinc oxide is widely been used to treat different skin conditions such as itching due to diaper rash and acne etc. It is also used in anti-dandruff shampoos and antiseptic ointments [15,16]. ZnO is broadest spectrum UVB and UVA absorber [17] which is consented by the U.S Food and drug administration (FDA) for used as a sunscreen. ZnO sunscreens are believed as nonallergic and non-

comedogenic. Ciprofloxacin is an antibiotic, often used to treat skin infections, typhoid fever, and urinary tract infections, ZnO nanoparticles are used to fasten the antibacterial activity of ciprofloxacin.

- ZnO is used in breakfast cereals as a necessary ingredient, as a source of zinc. Some packaged foods also contain a trace amount of ZnO even if it is not as an intended source of nutrients there. In the 2008 Chilean pork crisis, ZnO was associated to dioxin contamination. Zn white being highly opaque is used in paints as a pigment, although it is still less opaque than titanium oxide.
- Zinc white (ZnO) is also used in oil paintings. Its use in oil paintings is not new, it has been used in this since the 18<sup>th</sup> century. It is also used in mineral Makeup. ZnO when used in paints acts as a coating that has long been used as anticorrosive coatings for metals. For galvanized iron, it is effective like amazing. Fe is hard to protect because it reacts with organic coatings which result in a lack of adhesion and brittleness. But thanks to ZnO paints which retain the shine on such surfaces for many years [18]. Al doped ZnO, acts as a highly transparent and low resistive material, these properties make it useful in heat-protecting windows. These coatings let the visible part of the spectrum and reflect the infrared part [19]. Polyethylene naphthalene (PEN) is a plastic and can be protected using ZnO protective coating. This coating reduces the diffusion of oxygen with it [20].

## **1.4) Fundamentals of ZnO as a semiconductor:**

ZnO has some extraordinary properties which make it useful in semiconductor device applications. It has a wide bandgap and large free exciton binding energy due to which ZnO has always been in light of its semiconductor device applications. But somehow it has faced hindrance in its use due to a dearth of control over its conductivity. ZnO is always n-type and cause of it is in a considerable argument. Over the past few decades, there has been a huge improvement on this material, there is a voluminous betterment in the quality of ZnO single structure substrates. ZnO has captivated many research groups worldwide due to its likelihood of using it in complement to GaN or its alternative in optoelectronics; they are working hard to control its n-type conductivity. Theoretical studies have contributed a lot to deeply understand the effect of intrinsic and extrinsic

impurities on unintentional n-type conductivity in ZnO. However, achieving p-type doping is still challenging and key factors determining the stable p-type doping are still not determined.

#### **1.4.1) Advantages of ZnO over GaN:**

The handiness of large single crystals is the basic and notable advantage of ZnO. For instance, GaN is often produced on sapphire, with a lattice mismatch of around 16% which causes high concentration defects i.e ( $10^6$ -  $10^9$   $\text{cm}^{-2}$ ) [21]. ZnO shows better performance in photonic and electronic devices because the epitaxy of ZnO films on native substrates results in the ZnO layer with significantly less defects. ZnO is acquiescent to wet chemical etching which makes it feasible in fabrication and device design.

#### **1.4.2) Bandgap engineering of ZnO:**

Bandgap engineering of ZnO is accomplished by alloying it with CdO or MgO. The addition of Mg into ZnO increases the bandgap while Cd decreases it. CdO and MgO crystallize in the rock salt structure,  $\text{Mg}_{1-x}\text{ZnO}$  and  $\text{Cd}_{1-x}\text{ZnO}$  alloys in moderate concentration take the wurtzite structure of original compound, leading to a noteworthy change in the bandgap of ZnO.

There has been a basic issue in ZnO to control its conductivity. A very small amount of impurities (down to  $10^{-14}\text{cm}^{-3}$  or 0.01 ppm) and native point defects can affect the optical and electrical properties of materials. So, evaluating the part of native point defects i.e. vacancies, antisites, and interstitial defects is important and crucial. It has been postulated for a long time that the presence of oxygen vacancies or zinc interstitials are the causes of unintentional n-type conductivity in ZnO. The recent state of the art density functional calculations on high-quality ZnO crystals have proved that this attribution cannot be correct. Oxygen vacancies act as deep donors, so they can not be the cause of n-type conductivity. It was found that other point defects such as Zn antisites and interstitials are also very improbable causes of n-type conductivity in ZnO [32-37].



## 1.5) Doping and defect chemistry in ZnO:

### 1.5.1) Intrinsic Defects:

Intrinsic or native point defects are the disfigurements in the crystal structure having involved constituent elements only. Native defects could be of many types but basically, they include vacancies, interstitials, and antisites. In the case of ZnO if we would define all of these defects it will be like; Interstitial defect arises due to the presence of extra atoms replacing interstices in ZnO. A vacancy is formed when a certain atom is missing at the regular lattice position of ZnO, and antisites can be defined as the presence of a Zn atom on O lattice site or vice versa. Native defects can persuade the optical as well as electrical properties of a material. They have a strong effect on changing minority carrier lifetime and luminescence efficiency of a semiconductor, also these defects are involved in diffusion mechanisms connected to device degradation and growth [31-33].

Therefore knowing the behavior and incorporation of these defects in ZnO is mandatory for its impactful application in the semiconductor industry. Figure 1.2 shows the major defect types which are present in single-crystal ZnO, all of them are not supposed to be shallow defects.  $O_i$ ,  $V_o$ ,  $Zn_i$ , and  $V_{zn}$  are oxygen interstitial, oxygen vacancy, zinc interstitial, and zinc vacancy respectively. 'X' is an impurity atom, which can occur either as substitutional  $X_{zn}$  or interstitials  $X_i$  and  $X_o$  on oxygen and zinc sites respectively. A and D are the impurities i.e acceptor and donor respectively.

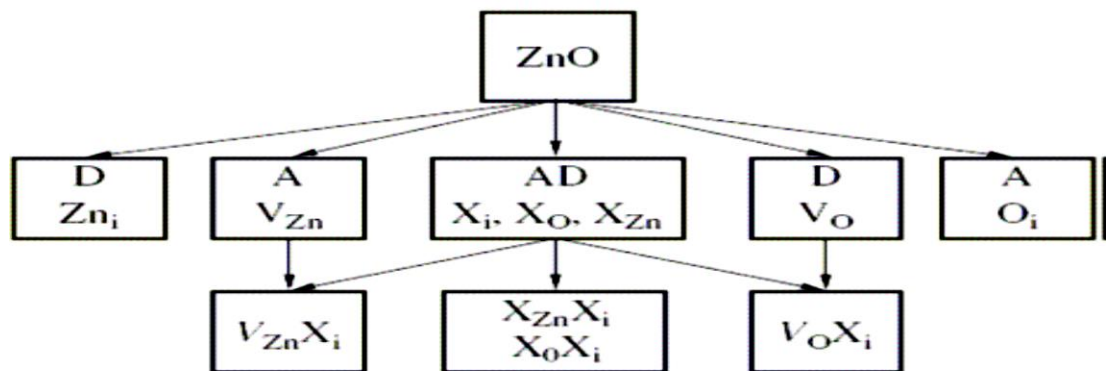
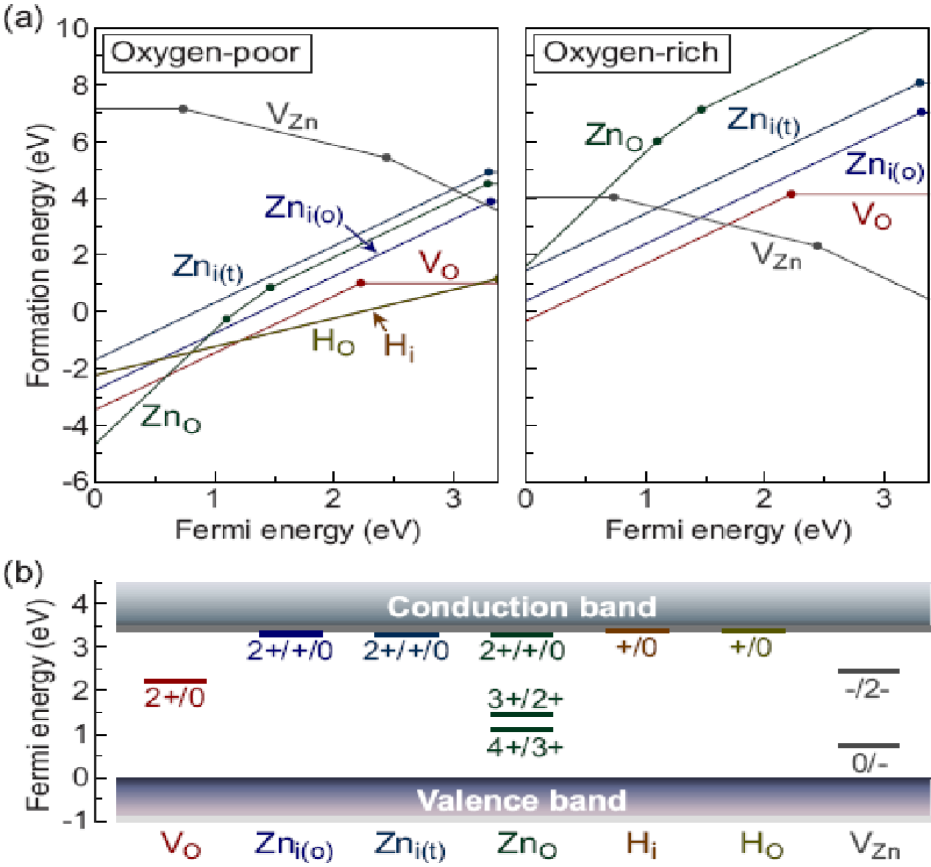


Fig 1. 2 Types of defects that may occur in ZnO

In ZnO, migration of energy is an important feature for native point defects. The migration energy entertains a major role in two types of diffusions, i.e impurity and modeling self-diffusion ( $E_s$ ). The relation of these energies is given as  $E_s = E_f + E_b$ , in other words, energy for modeling self-diffusion is the sum of formation energies of defects ( $E_f$ ) and migration energy ( $E_b$ ). The formation energy of defects depends upon experimental values for instance where the Fermi level is located and chemical potentials of oxygen and zinc. The difference of saddle point with migration route & configuration of equilibrium is known as the migration energy barrier, where the configuration of equilibrium can be projected with high quality of accurate principle calculations.

If defect level is expected at room temperature (RT), and is thermally ionized, the transition level for this is known as shallow level. If it is not ionized at RT, it is known as deep level.



**Fig1. 3 a) Formation energy of defects in ZnO in Oxygen rich and poor environment  
b) relative fermi energy [6]**

The formation energy of all the defects is shown in above figure, as it can be seen from it that zinc vacancies have the lowest formation energy in oxygen poor conditions and  $V_O$ (oxygen vacancy) has the lowest formation energy in oxygen rich environment. So it is more likely that in O poor environment Zn vacancies have more probability of occurrence and vice versa.

## **1.5.2) Doping in ZnO:**

Just like any other semiconductor, in ZnO there exists two type of dopings i.e p-type and n-type doping.

### **1.5.2.1) Acceptor Impurities:**

Those semiconductors which have a wide band gap energy it is very hard for them to achieve p-type doping. In case of ZnO when we talk about native point defects it is well established that both zinc vacancy and oxygen interstitials are known to behave as acceptors. But, it is very hard for these defects to create a shallow acceptor level. In literature we see that P-type doping in ZnO can be introduced by doping it with group I elements such as Li, K and Na which act as shallow acceptors for Zn site. Group V elements are also expected to introduce p-type doping in ZnO on Oxygen site but they act as deep acceptors. So, group I elements are believed to be better p-type dopants. Group I elements have comparatively small atomic radii so instead of substitutional sites interstitial sites are occupied by them in ZnO lattice. Because of this their expected behavior to act as acceptors get lost somehow and they behave as donors. Group I elements like Na and K have a larger bond length as compared to Zn-O bond length that is  $1.93\text{\AA}$ . Due to comparatively larger bond length they may form native defects in ZnO such as vacancies which compensates shallow acceptor doping. Likewise in group V elements there is likelihood of making antisites in ZnO to get rid of lattice strain due to their larger bond length like group I. They have tendency to substitute both Zn and O atoms and behave as donors in this situation. Nitrogen on the other hand has a smaller

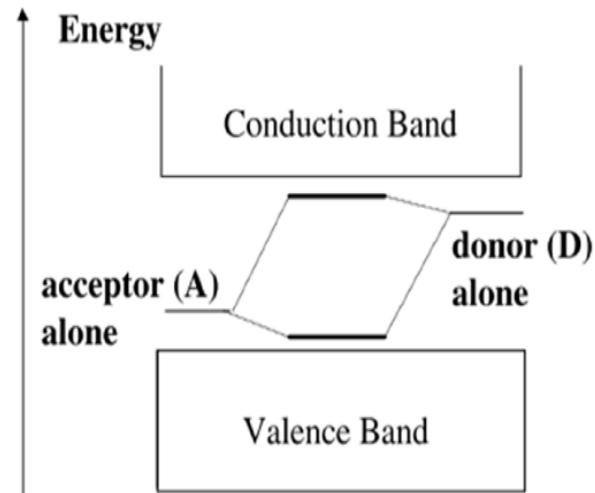
ionization energy so it can be used as a better candidate for shallow p-type doping and this type of doping can be attained by ion implantation method.

### 1.5.1.2) Donor Impurities:

As we know that ZnO is a n-type semiconductor intrinsically. It is assumed that in ZnO Oxygen vacancies and Zinc interstitials are dominant native donors. Under Hall effect measurements and photoluminescence it is expected that zinc interstitials are most expected candidates for shallow donors. When group III elements such as Al, Ga and In etc are substituted on Zn site they behave as shallow donors. These impurities have effective mass state near CBM at low temperature and their extra valence electrons are loosely bound. These extra electrons move to conduction band as temperature rises. Zhang et al calculated ionization energy of Al that is 120meV and it has a low formation energy[31]. Hu and Gordan[56] managed to get carrier concentration up to  $8 \times 10^{20} \text{cm}^{-3}$  with Al doping in chemical vapor deposition of ZnO. Indium and Boron also have been used as a donor in ZnO[57,58].

#### *Co-doping in ZnO:*

ZnO has a wurtzite tetrahedral structure in which every Zn atom is coordinated by four O atoms. ZnO has always been in light due to its semiconducting properties which is due to its n-type behavior which originates from its n-type behavior due to some native defects present in it or due to substitutional H impurities. Any non-divalent dopant results in instable ionic charge distribution in the crystal structure of ZnO. This can retard the dopant substitution in the lattice structure and can create more native defects. So basically co-doping model is adopted in ZnO in terms of charge compensation.



## 1.6) Role of interstitial and substitutional H in n-type conductivity:

It is established that the cause of unintentional n-type behavior of ZnO is due to the fusion of impurities which behaves as shallow level donors i.e hydrogen. As H is always there in all environments in which crystals are grown so there are huge chances of its acting as an impurity in ZnO. With the help of density functional theory (DFT), it has been revealed that interstitial H forms a bond with the shallow donor. Interstitial H is found in ZnO [38-40]. As interstitial H is highly mobile so it can diffuse easily, but ZnO shows n-type conductivity even at higher temperatures where the existence of interstitial H is very improbable, so there arises the difficulty. In a very recent study, it is found that H can replace O in ZnO and still acts as a shallow donor [36]. As substitutional H is more stable than interstitial H so it explains the validity of n-type conductivity even at high temperatures and its variation with partial pressure[36]

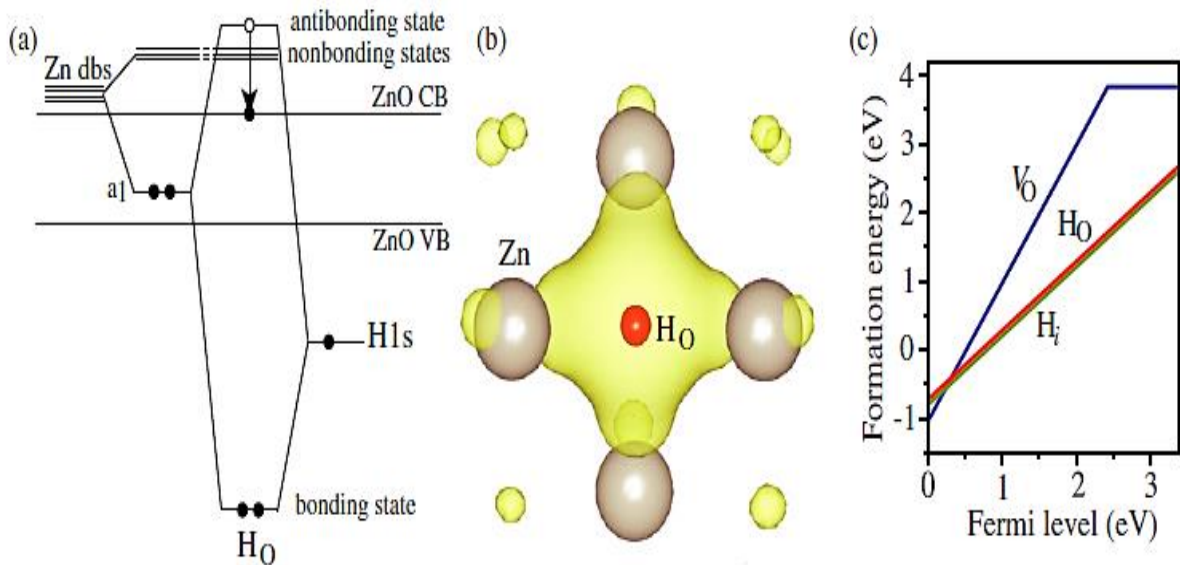


**Fig 1. 4 This shows Coupling among H 1s orbital and Zn 4s dangling bonds (Zn dbs) to make the H multicenter bond in ZnO [30]**

## ***Scaling of the devices:***

Integrated circuits are very crucial in every electronic device. Metal oxides semiconductor field-effect transistors (MOSFET) are believed as the elementary building block of new technology. The electronic industry is working hard to scale down the devices according to Moore's Law [27]. This law states that, in every two years number of transistors on an IC get doubled i.e performance efficiency will also be doubled.  $\text{SiO}_2$ , which has lately been used in MOSFET's has reached its critical restrictions, so it is need of the hour to engineer materials with high dielectric constant ( $k$ ) to scale the devices according to Moore's Law.

### **1.7) Introduction to dielectric material**

By applying an external electric field a dielectric material can be polarized. When a dielectric is kept in the vicinity of an external field (i.e electric) the electric charges do not flow like they do in conductors but they slightly move from their equilibrium position and produce an effect known as dielectric polarization. Due to this polarization the positive charges move in the direction of field and negative charges move against to that field which in result creates an internal field that somehow reduces the total field of the dielectric. Dielectrics are crucial for many phenomena in solid state physics, optics and electronics etc.

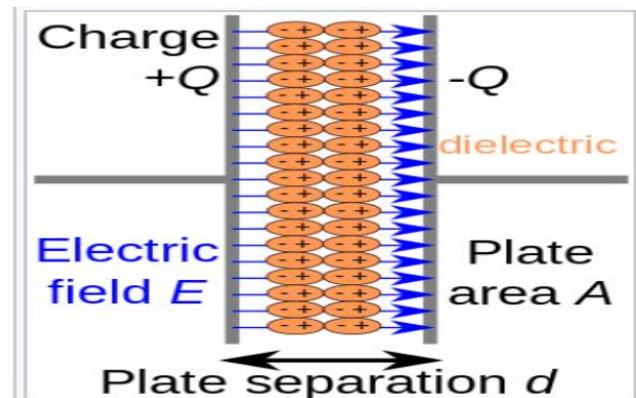


**Fig1. 5 A polarized dielectric material (parallel plate capacitor)**

In the **classical approach to dielectric model** any material is composed of atoms and every atom has a positive point charge at its center circumscribed by negative charge I,e electrons. When an electric field is applied this cloud gets distorted as shown in the figure.

This gets reduced to simple dipole using the superposition principle. A dipole is characterized by a vector quantity known as dipole moment shown as a blue arrow in the figure and denoted by  $M$ . Note that here in this particular example the dipole moment is pointed to the same direction as electric field but its not the case always, its just simplification here that is right for most of the materials.

When the external electric field is removed the atoms turned to its actual original state and the time they take in this process is known as relaxation time, an exponential decay. This is just a simplified model. The behavior of a dielectric varies from situation to situation. The more complicated the situation is the richer the model gets.

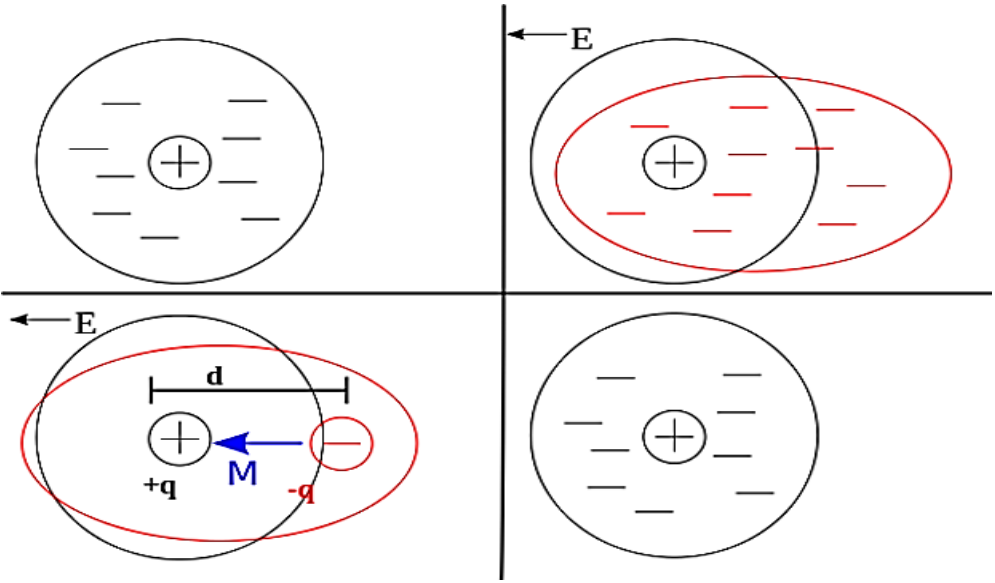


**Fig 1. 6 behavior of an atom under applied electric field**

### *The important questions could be:*

- Does the electric field vary with time, if so then at what rate?
- Does that behavior depend on isotropy of the material?
- Are there nonlinearities in the expected response?
- Does any interface or boundary need to be taken in account?

The relationship between electric field  $\mathbf{E}$  and dipole moment  $\mathbf{M}$  for a particular material can be described by the function  $F$ , as following

$$\mathbf{M} = F(\mathbf{E})$$

One chooses the function  $F$  when relation between  $\mathbf{E}$  and  $\mathbf{M}$  are known and defined which correctly depicts the phenomena of interest.

#### **1.7.1) Dielectric constant:**

For a material to compete SiO<sub>2</sub> it must possess a dielectric constant greater than 5 [28].

The Clausius Mosotti equation for dielectric constant is;

$$k = \frac{3V_m + 8\pi\alpha_D^T}{3V_m - 4\pi\alpha_D^T}$$

Here  $V_m$  is the molar volume and  $\alpha_D^T$  is the Total Dielectric Polarizability. Whereas  $V_m$  can be obtained by the following equation;

$$V_m = l_1 l_2 l_3 \frac{\sqrt{1 - \cos^2 \alpha - \cos^2 \beta - \cos^2 \gamma + 2 \cos \alpha \cdot \cos \beta \cdot \cos \gamma}}{Z}$$

$l_1, l_2,$  and  $l_3$  are lengths of the unit cell and  $a, b, c$  are interaxial angles and  $Z$  shows the no of formula units per unit cell.

To find total polarizability additive rule is applied



$$\alpha_D^T = \sum_{j=1}^n V_j \alpha_D(j)$$

n is the total number of ions.  $V_j$  represents the number of ions of the type j.

The static dielectric constant of oxides is calculated by the following equation

$$k = n^2 + \frac{Ne^2Z^*{}^2}{m\omega_{T0}^2}$$

where “n is the refractive index,  $Z^*_T$  is a transverse effective charge.

### 1.7.2) Dielectric Polarization:

When a dielectric material is placed in an external electric field it gets polarized. There are many type of dielectric polarizations, some of them are

- Space polarization
- Electronic polarization
- Dipolar polarization
- Ionic polarization

If a dielectric material has n no of atoms per unit volume and each atom/molecule is polarized then one can write;

$$P = n(q \times d) = n \times \mu$$

If a capacitor has a total charge density  $\sigma$  then the free charge density  $\sigma_f$  will be  $\sigma - \sigma_b$ . A flux density is created due to this free charge and which by using Gauss’s law is written as;

$$D_0 = \epsilon_0 \times E$$

The total dielectric flux density is written as

$$D = P + D_0$$

Also

$D = \epsilon \times E$  so above equation becomes;

$$P = (\epsilon - \epsilon_0)E$$

The relationship between applied electric Field E and Polarization P is described by another important factor known as dielectric susceptibility ( $\chi_e$ )

$$P = \chi_e \epsilon_0 E$$

The comparison of the above two equations give us ;

$$\chi_e = \frac{(\epsilon - \epsilon_0)}{\epsilon_0} = (\epsilon_r - 1)$$

So the equation for P becomes,

$$P = (\epsilon_r - 1) \epsilon_0 E$$

So, it can be written as,

$$\chi_e = P/D_0$$

So,  $\chi_e$  **the electric susceptibility** represents the ratio of bound surface charge density to free surface charge density. It also measures that how easily a dielectric material polarizes in response to an electric field.

Generally a material can't get polarized instantaneously so a more general formulation as a function of time is represented as;

$$P(t) = \epsilon_0 \int_{-\infty}^t \chi_e(t - t') E(t') dt'$$

It says that Polarization is a convolution of the applied electric field at previous times and time dependent susceptibility is given by  $\chi(\Delta t)$ . The upper limit can extend to infinity if we define  $\chi(\Delta t)=0$  for  $\Delta t < 0$ .

## Chapter 2: Synthesis and Literature Review

---

### 2.1) Synthesis Method:

There are different approaches for the synthesis of ZnO. In this research work, Sol-gel synthesis of ZnO is adopted.

#### 2.1.1) Sol-Gel:

Sol-gel is believed as the cheapest method for the synthesis of ZnO or any other metal oxide. It is a very environmentally friendly method. In a sol-gel method as the name suggests there is the formation of a gel which after drying results into desired metal oxide. Following is the flow chart of the method. Fig 2.1

#### Detail of the process:

First of all colloidal solution is prepared by using sol precursors in the form of metal ions. Because of radical hydrolysis, metal alkoxides possess significant importance. Titanes, aluminates, and borates can also be used as precursors for sol-gel synthesis. Some of the precursors don't do hydrolysis readily due to their immiscibility in water, to overcome this problem a mutual solvent such as alcohol is used. The sol-gel method comprises of the following four steps

**-Hydrolysis:** First of all hydrolysis of the precursors is done. In this step, a catalyst could be used to enhance the hydrolysis process. Basic medium ( $\text{NH}_3$  or  $\text{NaOH}$ ) or acidic medium ( $\text{CH}_3\text{COOH}$  or  $\text{HF}$ ) can be used as a catalyst.

**-Condensation:** Next step is a condensation of the solution.

**-Growth:** When condensation is done, particles start to grow, this growth depends upon various parameters such as pH of the solution, temperature, and pressure.

**-Gel Formation:** Once the growth is done, particles start to agglomerate and results in a thick gel.

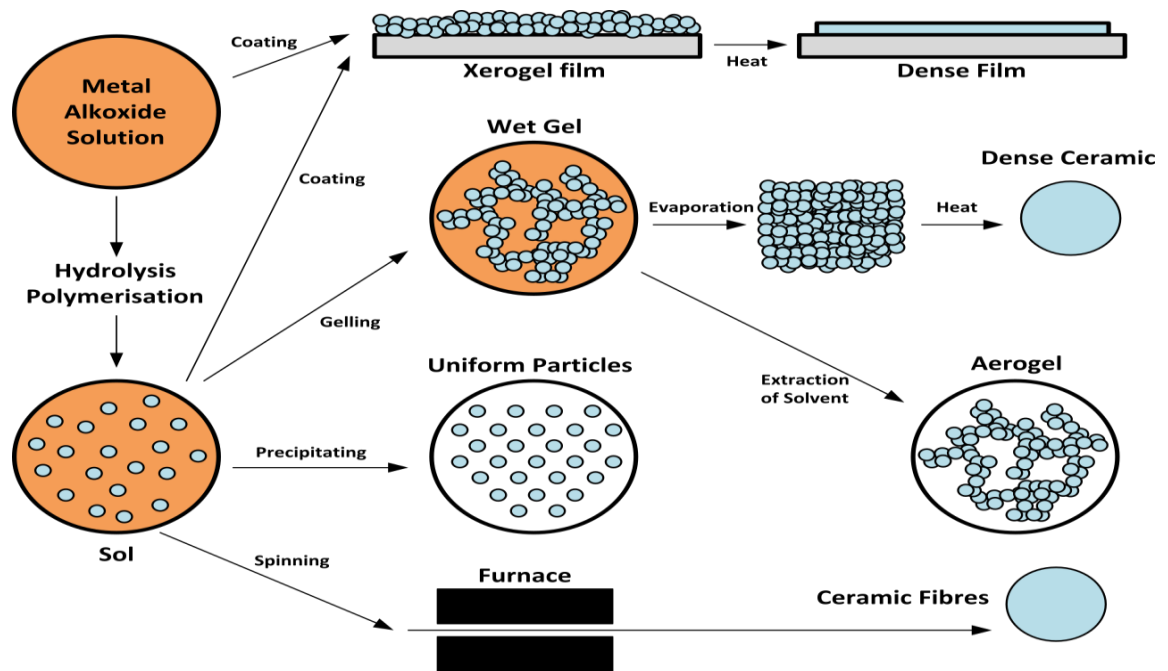


**Fig 2. 1 Illustration of Sol gel method**

### 2.1.2) Apparatus used in the sol-gel method:

The apparatus which was used for the synthesis includes:

- Magnetic stirrer
- Hot plate
- Digital balance
- pH paper
- Crucibles
- Drying oven
- Muffle furnace
- Mortar and pestle

Magnetic stirrer and hot plate warrants that liquid samples are homogeneous inconsistency. A magnetic stirrer uses magnetic stirrer bars to complete the mixing process. The digital mass balances in the labs are very sensitive instruments used for weighing substances to the milligram (0.001 g) level. Digital mass balance was used for weighing precursors and dopants used in the synthesis. pH papers tell about the pH level of the solution. They were used during synthesis to confirm the pH of the solution when the reducing agent was poured into the precursor. Drying oven was used for drying Zn(OH)<sub>2</sub> gel. It was normally settled at 60<sup>0</sup>C and samples were placed in it overnight for drying. It is always a safe option to set the temperature of a drying oven less than the boiling temperature of the water or whatever solvent has been used. Crucibles are used for heating a material at a very high temperature because they are made up of the substance which can bear high temperatures. Aluminum crucibles were used for placement of samples into muffle furnace for calcination. They worked well and didn't melt even at very high temperatures. A Muffle Furnace is used for high-temperature Applications for example it facilitates researchers to determine what proportion of the particular sample is nonvolatile or non-combustible. Typically a muffle furnace can achieve temperatures up to 1,800<sup>0</sup>C which helps in facilitating sophisticated metallurgical applications. It was used for changing the phase of samples i.e Zn(OH)<sub>2</sub> into ZnO, which is called calcination.

## **2.2) Synthesis of undoped and Er, Cu- doped ZnO:**

For synthesis following chemicals were used;

- Zinc Nitrate Hexahydrate Zn(NO<sub>3</sub>)<sub>2</sub>.6H<sub>2</sub>O
- Sodium Hydroxide(NaOH)
- Copper Sulphate(Cu(SO<sub>4</sub>)<sub>2</sub>)
- Erbium nitrate pentahydrate Er(NO<sub>3</sub>)<sub>3</sub>.5H<sub>2</sub>O
- Distilled Water

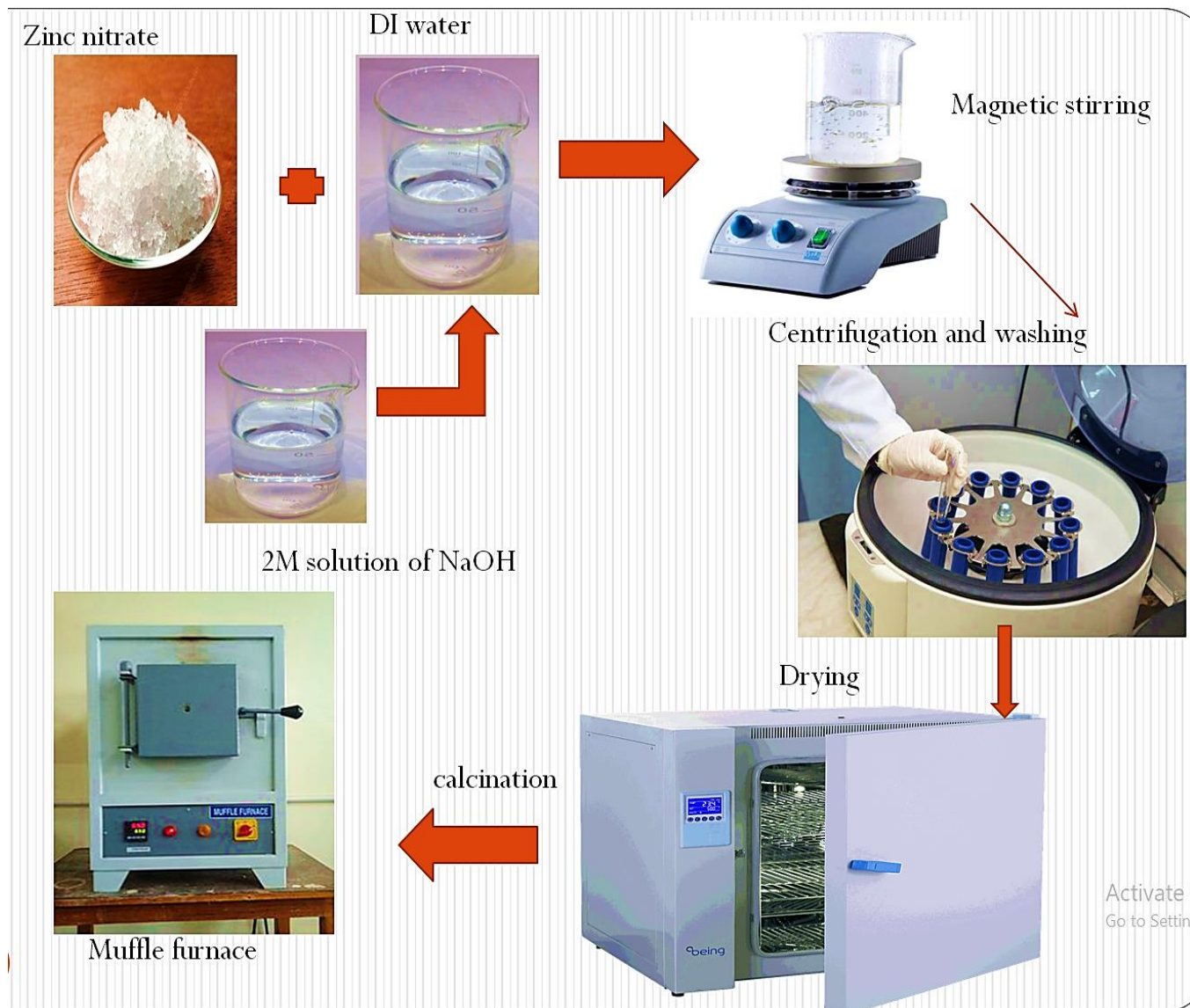
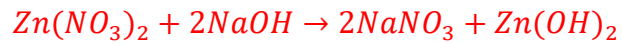


**Fig 2. 2** A visual representation of the process of synthesis

### 2.2.1) Undoped ZnO:

For the preparation of undoped ZnO, Zinc Nitrate Hexahydrate  $Zn(NO_3)_2 \cdot 6H_2O$  from Sigma Aldrich was used as a precursor. Distilled water was used as a solvent. NaOH purchased from Sigma Aldrich was used as a reducing agent.

**Reaction equation:**



### Procedure

1M solution of  $Zn(NO_3)_2 \cdot 6H_2O$  (14.874075g) was prepared in 50ml DI water and placed on a hot plate for stirring for half an hour. 2M NaOH solution prepared in 50ml DI water was added dropwise in the solution of zinc nitrate. After the addition of NaOH, the solution turned into a thick gel. This gel was centrifuged using a centrifuge machine. Washing of the gel was done several times by centrifugation with DI water. The washed gel was placed into a drying oven overnight for drying. Dried  $Zn(OH)_2$  was then calcined using a muffle furnace for 4 hours at  $450^{\circ}C$ . A very fine powder of ZnO was obtained after calcination which was pure white.

### 2.2.2) co-doped ZnO:

Four CO-Doped samples of ZnO were synthesized using the sol-gel method. The dopants were Erbium and Copper. They are 0.25,0.5,0.75 and 1% Er,Cu doped ZnO. Erbium behaves as an n-type dopant and copper as a p-type dopant in ZnO. Later in XRD results, it will be shown that it is successfully doped into ZnO's substitutional sites. For doping purpose **Erbium nitrate pentahydrate  $Er(NO_3)_3 \cdot 5H_2O$**  from sigma Aldrich was purchased. Copper's precursor was **copper sulfate**. All the chemicals were of research-grade and 99% pure.

For the preparation of 0.25,0.5,0.75 and 1% Er, Cu doped ZnO the same procedure was followed as described for undoped ZnO earlier in this chapter.

## **Procedure:**

For the preparation of 0.25%, co-doped ZnO 0.0099755g copper sulfate was dissolved in 0.0625ml DI water and 0.028834g Erbium nitrate was dissolved in 0.0625ml DI water. Another solution of zinc nitrate was prepared by dissolving 1M Zn(NO<sub>3</sub>)<sub>2</sub> i.e 7.40814g of it in 24.875ml DI water. This solution was placed for stirring and after 15 minutes 0.0625 molar solution of Erbium nitrate and copper sulfate which was earlier prepared was added into it and left for stirring for another 15 minutes. Once the stirring is done 2M NaOH solution was added dropwise which turned the solution into a gel. This gel was then washed with DI water several times using a centrifuge machine and placed for drying in a heating oven. The dried gel was then calcined in a muffle furnace for 4 hours at 450°C. A grayish powder was obtained and saved for characterizations into glass vials. For preparation of 0.5,0.75 and 1% co-doped ZnO 0.0199g,0.0299g,0.0399g copper sulphate was added in 0.025,0.1875 and 0.25ml DI water respectively and 0.0576g,0.0865g and 0.1153g Erbium nitrate was dissolved into 0.025,0.1875 and 0.25ml DI water respectively. These solutions were then added into Zinc nitrate solution and afterwards same procedure was followed as above. All of the samples obtained were finely ground using mortar and pestle and saved into glass vials for XRD, DRS, and dielectric measurements.



## 2.2 Literature Review and Background:

As it is well established, that dielectric materials having colossal dielectric permittivity have drawn humongous attention due to their utter need in device miniaturization and their usage in energy storage systems. They have been used in multi layer capacitors from decades. To date there have been many materials in which CP (permittivity larger than  $10^3$ ) is discovered [49-53]. One of them are  $\text{BaTiO}_3$  based pervoskite materials in which CP is attributed to a very well known phenomenon known as Internal barrier layer capacitance (IBLC) [49]. They observed CP up to 1600 in this particular work which was published back in 2006. According to them the reason behind achieving CP in this material is related to the ferroelectric behavior because its dielectric constant varies with temperature and almost linear polarization hysteresis loops are observed that is the characteristic of ferroelectric materials [49].

In materials like  $\text{CaCu}_3\text{Ti}_4\text{O}_{12}$  [50] and (Li, In) co doped NiO [51] the same reasoning for the CP has been given that is IBLC effect. As we know that, doping can change a material drastically. So is the case with CP. It has been observed that doping plays a significant role in understanding and obtaining CP in many materials such as in doped NiO and in transition metal oxide CuO. **Electron pinned defect dipoles (EPDD) and co-doping:**

There is an advanced recent development in achieving colossal dielectric permittivity using a mechanism known as electron pinned defect dipoles that explains the ultimate cause of CP in In(acceptor) and Nb(donor) co-doped  $\text{TiO}_2$ [53]. The material possesses the CP on the order of  $10^4$  with very low dielectric loss i.e less than 0.05 with splendid thermal and frequency stability. W.Hu et al proposed that the cause of CP in this material originate from coupled triangular and diamond shaped defect clusters. Such defect clusters has a promising ability of colossal permittivity and low dielectric loss. The materials belonging to such cast of materials have a potential to be used in new generation capacitors due to their frequency and temperature

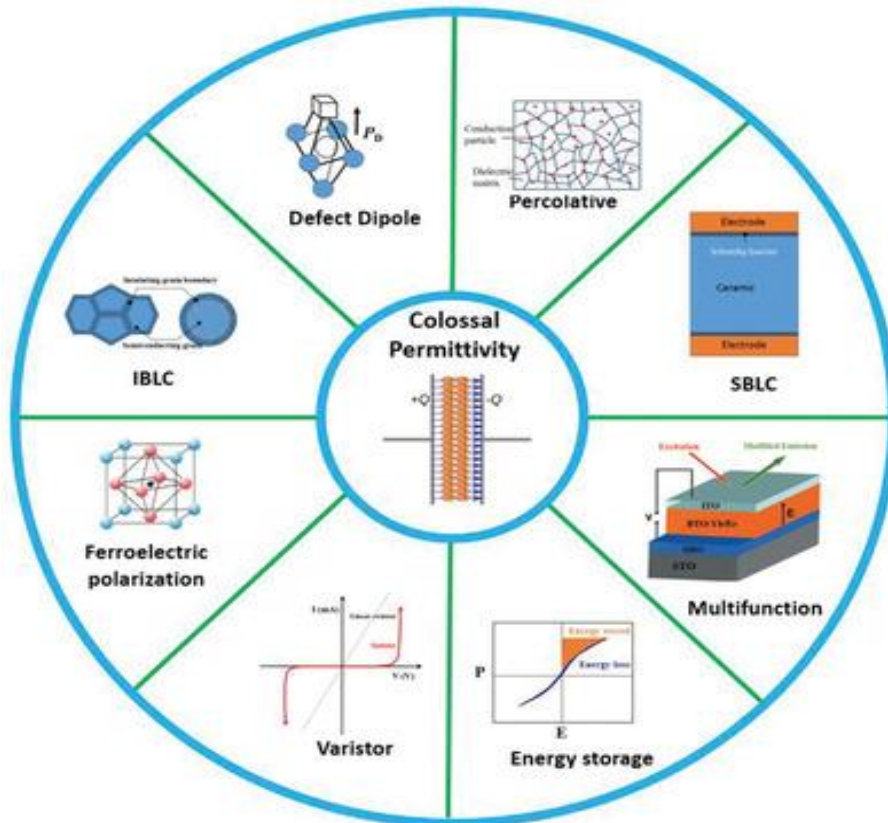
independent CP behavior. So, it is need of the hour to conduct a thorough research for new acceptor/donor co-doped rutile materials.

**ZnO as a CP material:**

The doors for using ZnO as a CP material opens up with the successful accomplishment of colossal permittivity in Mg doped ZnO which reaches up to  $10^4$  [54] indicating that ZnO could be another propitious material for attaining CP. That is very new field of research on ZnO so a very novel and less successful literature is available on that.

**Co-doping in ZnO:**

ZnO has a wurtzite tetrahedral structure in which every Zn atom is coordinated by four O atoms. ZnO has always been in light due to its semiconducting properties due to its n-type nature which originates from its n-type behavior due to some native defects present in it or due to substitutional H impurities. Any non-divalent dopant results in instability of ionic charge distribution in the lattice structure of ZnO. This can further retard the dopant incorporation in the lattice structure and can create more native defects. So basically co-doping model is adopted in ZnO in terms of charge compensation.



**D. Huang et al** reported the successful doping of Li and In into ZnO i.e  $[Zn_{(1-2x)}(Li,In)_xO]$  when  $x=0.5\%$  and observed a colossal permittivity up to 3800 with very low tangent losses of 0.11 at 1kHz frequency[55]. They used Electric modulus spectroscopy and impedance analysis to know the cause of CP in the material. In the temperature range of 293K-363K two relaxation peaks were observed which according to Debye relaxation theory points out that these relaxation peaks are attributed to doubly and singly charged oxygen vacancies created due to successful incorporation of Li and In into ZnO lattice. This reveals that oxygen defects are the main causes of CP in Li, In co doped ZnO[55]. There is very little literature available on ZnO to be used as host material doped with donor and acceptor impurity for the accomplishment of high dielectric permittivity. As described, In  $TiO_2$  ceramics there is successful achievement of CP that is temperature and frequency independent but in ZnO it hasn't yet been reported.

In this work we have successfully doped Erbium and copper into ZnO substitutional sites which is confirmed from XRD. **Erbium** has been used as a donor and **copper** as an acceptor material. We will discuss its Impedance analysis and some other morphological properties in results section.

# Chapter 3: Characterization Techniques

---

After the preparation of samples, the next step is to characterize the samples to know its morphology i.e structural and compositional analysis. Many characterization techniques have opted in experimental condensed matter physics for characterization of materials, few of them which are used in this research work for the characterization of samples are listed below,

- **X-ray Diffraction(XRD)**
- **Diffuse Reflectance Spectroscopy(DRS)**
- **Impedance Spectroscopy(IS)**

XRD and DRS are utilized for confirmation of the successful synthesis of the prepared samples while Impedance spectroscopy helped us to measure the dielectric properties of the samples which is the main part of this research work. So, much of the focus will be given to Impedance spectroscopy and we will learn in this chapter about the physics behind IS so that we can interpret our IS results correctly.

## **3.1) X-ray Crystallography:**

Electromagnetic radiations are considered as waves of electromagnetic field which propagates through space and carries electromagnetic energy. In the early part of the last century, science has made every effort to investigate every bit of detail about its frequency, wavelength, speed, and energy, etc. Depending upon the wavelength and frequency of oscillation an electromagnetic wave is characterized within the electromagnetic spectrum. The electromagnetic spectrum includes radio waves, microwaves, infrared radiation, visible light, ultraviolet radiation, X-rays and gamma rays if they are arranged in order of increasing frequency and decreasing wavelength. X-rays have their class among electromagnetic radiations, mostly due to their huge applications and method of production. X-rays are produced in cathode ray tubes, a heated filament is used as a source for electrons and a high potential is used to accelerate them.

### **3.1.1) X-ray Powder Diffraction Instrumentation:**

## How does it work?

X-ray diffractometers comprise of three main components; an X-ray tube, Sample holder, and Detector. Generation of X-rays is done in a cathode ray tube, they are produced by heating a filament which results in the production of electrons, and they are then accelerated towards a target by applying a voltage. When these electrons have enough energy to extricate inner shell electrons of the target material, the characteristic spectra of X-rays are emitted. These spectra consist of several components, the famous one is;  $K_{\alpha}$  &  $K_{\beta}$



**Fig3. 1 Advance D8 XRD machine**

$K_{\alpha}$  consists of  $K_{\alpha 1}$  and  $K_{\alpha 2}$ .  $K_{\alpha 1}$  has a shorter wavelength than  $K_{\alpha 2}$  but its intensity is greater. Different target materials (Cu, Fe, Mo, Cr) produce different wavelengths. For diffraction monochromatic X-rays are required, so filtering by coils or monochromators is done for obtaining monochromatic X-rays. Copper is considered as the finest target material for single crystal diffraction having  $CuK_{\alpha}$  radiation  $=1.5406\lambda$

### 3.1.1) Fundamental Principle of X-ray Powder Diffraction:

In 1912, Max von Laue proposed that crystalline materials act as a diffraction grating for X-ray wavelengths. X-ray diffraction now is a very important as well as common technique for studying crystal structures i.e about their atomic spacing etc. It is based on the principle of constructive interference between monochromatic X-rays and crystalline samples.

#### Bragg's Law:

Through the association of incident rays of X-rays with the sample constructive interference is achieved when Bragg's condition is satisfied i.e

$$n\lambda = 2d\sin\theta$$

This law basically relates the  $\lambda$  of X-ray radiation to diffraction angle and lattice spacing 'd' in a crystalline material.[41]

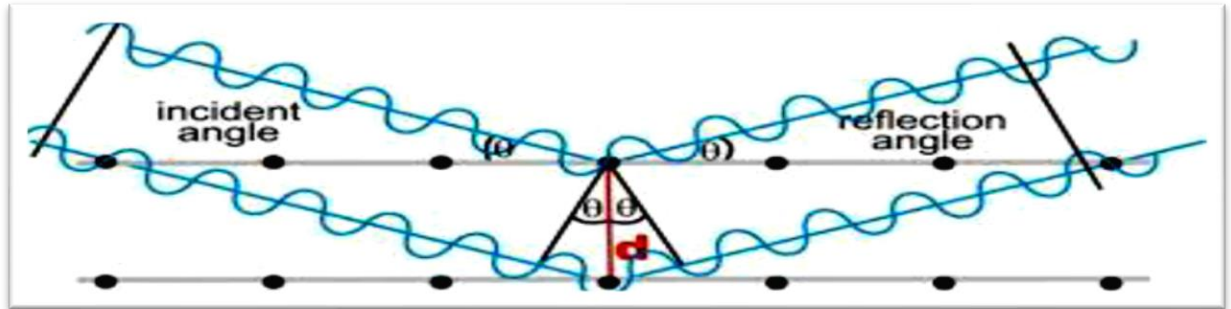


**Fig3. 2 Illustration of Bragg's Law [42]**

These diffracted X-rays are detected, processed, and analyzed afterwards. Every material has a unique set of d-spacings and by converting diffraction peaks to d-spacings a particular material is identified.

### **3.2) Diffuse Reflectance Spectroscopy (DRS):**

Before going into the details of Diffuse Reflectance Spectroscopy, let's first define "Diffuse Reflection". In Diffuse reflection a ray which is incident on any surface gets scattered at more than one angle, it is different than specular reflection. In specular reflection, light is reflected at just one particular angle. Different materials behave differently when exposed to light, diffuse reflection is the property of certain materials for example non-absorbing powders like plaster reflects light diffusely with impeccable proficiency. Many substances reflect light both diffusely and specularly.

#### **3.2.1) Mechanism:**

Surface roughness is not the major cause of diffuse reflection in solids in general, although there is a requirement of flat surface for specular reflection this contributes nothing to DR. For instance a piece of marble which is highly polished will never turn

into a mirror no matter how much polished it is. Yes, polishing does produce some specular reflection but remaining has to have diffusely reflected in any way.



**Fig 3. 3 UV-Visible Diffuse Reflectance Spectrophotometer**

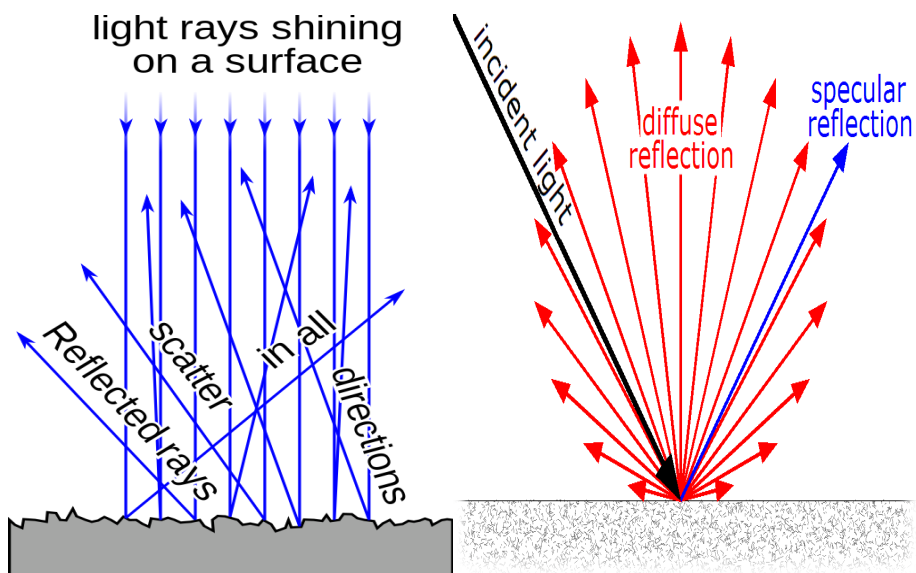


**Fig 3. 4 It is a depiction of diffuse and specular reflection from an absurd and glossy surface respectively.[43]**

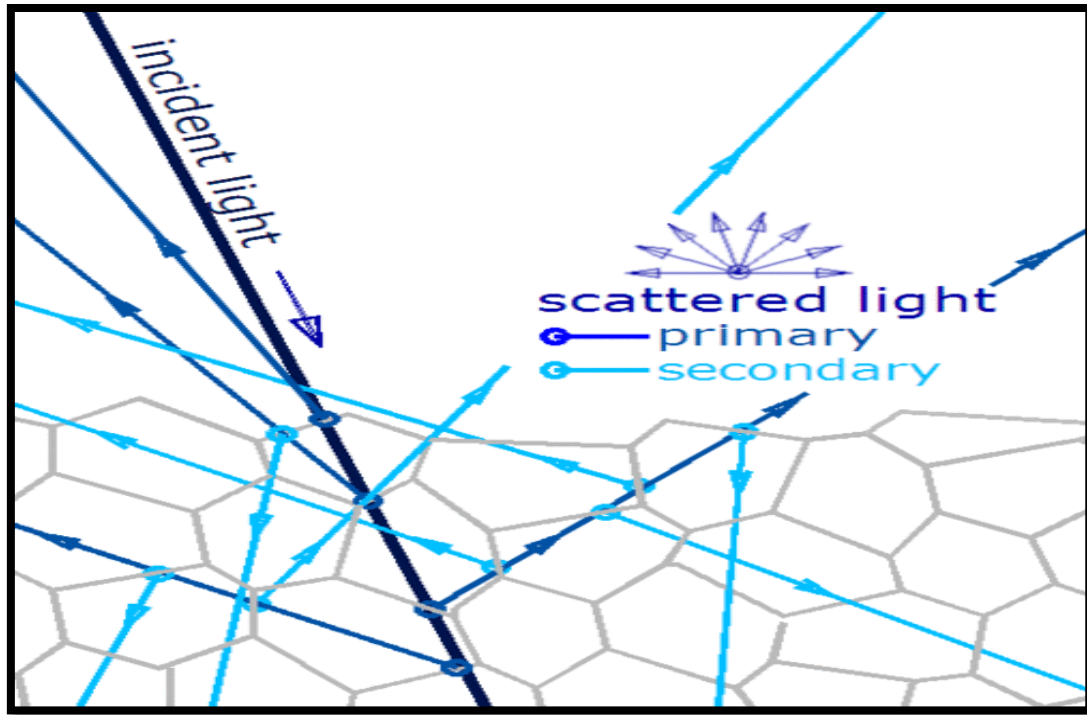


**Fig3. 5 Diffuse Reflection through a solid**

It is believed that most of the time DR has nothing to do with the surface but to the scattering centers under the surface [44] as manipulated in fig 3.5. Let us assume that this fig represents snow, and polygons are imagined to act as ice crystallites in this particular example. If a ray is partially reflected by the first particle and enters in it and then again reflected by the second particle and passes into it and intrudes on third and so forth producing series of “primary” scattered rays which through exact mechanism results into “secondary” scattered rays and so on. All of these rays make their journey to the snow crystallite which does not intend to absorb them and making their way to surface reflecting in arbitrary directions.



Well, a surface may reveal both Specular and diffuse reflection, for instance, glossy paints give a fraction of specular reflection whereas matte paints are solely diffusely reflective. Depending on the material reflection can be purely diffused or reflective or between them. Very few materials lack internal subdivisions due to which only subsurface scattering phenomenon occurs that results in specular reflection only. In Silver and Aluminum, there is only a specular reflection of light. All other materials generally do not give specular reflection more than a few percent.

### **3.2.2) Diffuse Interreflection:**

It is a process in which light reflected from one object strikes to other objects in its premises and illuminates them. It categorically describes the reflection of light from objects which are not so shiny such as grounds, walls, or fabric to get access to areas that are not directly given light. If we have a colored surface the reflected light will also be colored, which gives color to the objects in premises.

### **3.2.3) Kubelka-Munk(K-M) Treatment :**

Optical properties of powdered materials are recurrently determined through UV-Vis Spectroscopy by dispersing them in liquid media. Although the peak position of absorption can be found from it but accurate value of their band gap is almost impossible. Nonetheless, using Kubelka-Munk treatment on diffuse reflectance spectra by Diffuse reflectance spectroscopy (DRS) of such powdered nanomaterials, it is viable to obtain their  $E_g$  accurately. The theory which makes it feasible to use DR spectra was proposed by Kubelka and Munk [45]. Initially, they gave a model to determine the behavior of light into a light scattering specimen.

$$-di = -i(S + K)idx + Sjdx \quad ; \quad dj = -(S + K)jdx + Sidx \quad \mathbf{i}$$

$i$ =intensity of light traveling inside the sample towards its un-illuminated surface and  $j$ =intensity of light traveling inside the sample towards its illuminated surface,  $S$  and  $K$  are the so-called Kubelka- Munk(K-M) scattering and absorption coefficients respectively. This model is valid only if the particle size is comparable to the wavelength

of the incident light. Otherwise if the sample is infinitely thick supposedly then sample holder and width have no impact on Reflectance(R). For this Kubelka-Munk equation for any wavelength is;

$$\frac{K}{S} = \frac{(1-R_{\infty})^2}{2R_{\infty}} = F(R_{\infty}) \quad \text{ii)}$$

Where  $F(R_{\infty})$  is so-called K-M function and  $R_{\infty} = R_{\text{sample}} / R_{\text{standard}}$  [46].

The bandgap  $E_g$  and absorption coefficient “ $\alpha$ ” of a direct bandgap semiconductor in a parabolic band structure are related by the following equation [47].

$$\alpha h\nu = C_1 (h\nu - E_{gap})^{1/2} \quad \text{iii)}$$

here  $\alpha$  is the “linear absorption coefficient of the material”,  $h\nu$  is “photon energy” and  $C_1$  is the constant. When an object diffusely scatters the light then the K-M absorption coefficient  $K$  becomes  $K=2\alpha$ , For this, considering K-M scattering coefficient  $S$  as a constant and inducing remission function in eq(iii) following expression is obtained:

$$[F(R_{\infty})h\nu]^2 = C_2 (h\nu - E_{gap}) \quad \text{iv)}$$

As a consequence, getting  $F(R)$  from eq ii) and plotting the  $[F(R_{\infty})h\nu]^2$  against  $h\nu$ , the bandgap  $E_g$  of a powder sample can be excerpted easily.[46]

### 3.3) Impedance Spectroscopy (IS):

Impedance spectroscopy is a useful technique to investigate the electrical behavior of microcrystalline solid material with variable frequency and as a function of alternating current (ac). This technique measures the electrical properties of a material's interface attached to electrodes. Interaction between a sample and current takes place in three regions described in the figure below i.e i) at grain boundary ii) electrode's surface iii) inside grains

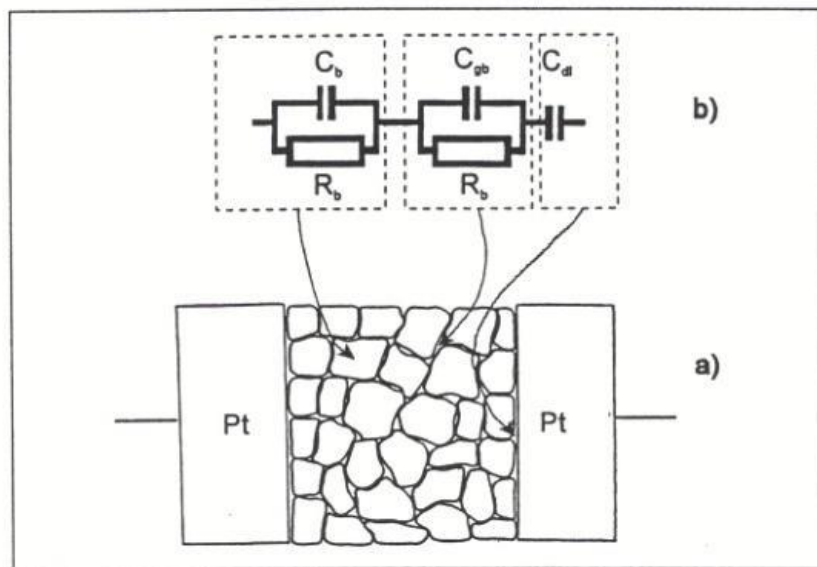


Fig 3. 6 Interactions at grains and grain boundaries

#### 3.3.1) Working principle of impedance:

Resistance of a material in ohms's law is defined as the ratio of applied voltage  $V$  to current  $I$ , whereas impedance of a material is a broader theory than resistance. Impedance is a broad circuit constraint because it also takes phase into account in complex circuits. The fraction of applied sinusoidal voltage to reaction current is known as Impedance.

$$\text{Imp} = V / I$$

By applying sinusoidal varying voltage perturbation, one can measure the impedance:

$$V(\omega) = V_0 \exp(i\omega t) \quad (3.1.1)$$

Where,  $\omega$  is known as angular frequency and  $V_0$  is amplitude of signal. With phase shift of the ac signal above equation becomes:

$$I = I_0 \exp(i\omega t + \delta) \quad (3.1.2)$$

Where, "I" is the response current and  $\delta$  is the phase angle. For the correspondence frequency the ratio of output by input determine the impedance in accordance with Ohm's law.

$$\begin{aligned} Z(\omega) &= V(\omega)/I(\omega) && \text{also,} \\ Z(\omega) &= \frac{V_0 \exp(i\omega t)}{I_0 \exp(i\omega t + \delta)} && \text{so;} \\ Z(\omega) &= Z_0 \exp(i\delta) && (3.1.3) \end{aligned}$$

With magnitude  $Z_0$ , impedance  $Z(\omega)$  is known as a complex number with  $\delta$  as phase shift. Its mathematical expression is written as;

$$Z(i\omega) = Z_0(\cos\delta + i\sin\delta) \quad (3.1.4)$$

The purpose of the precise values of both the phase and the magnitude of the impedance at every single frequency is to smooth the progress for capacitance, so that their values can be determined at each given frequency. For a clean resistor R, V and I both are in phase so the magnitude of Z will be;

$$|Z| = R$$

Whereas,  $Z(\omega)$  contains two parts including real as well as imaginary. Its Cartesian form is:

$$Z(i\omega) = R + iX$$

Where, R is known as real resistive part and X is the imaginary reactive/capacitive part of impedance,

$$Z^* = Z' + iZ'' \quad (3.1.5)$$

# IS: TECHNIQUE

Small ac signal ( $V \approx 10 \text{ mV}$ ) is applied to sample over a wide range of frequency (mHz to MHz)

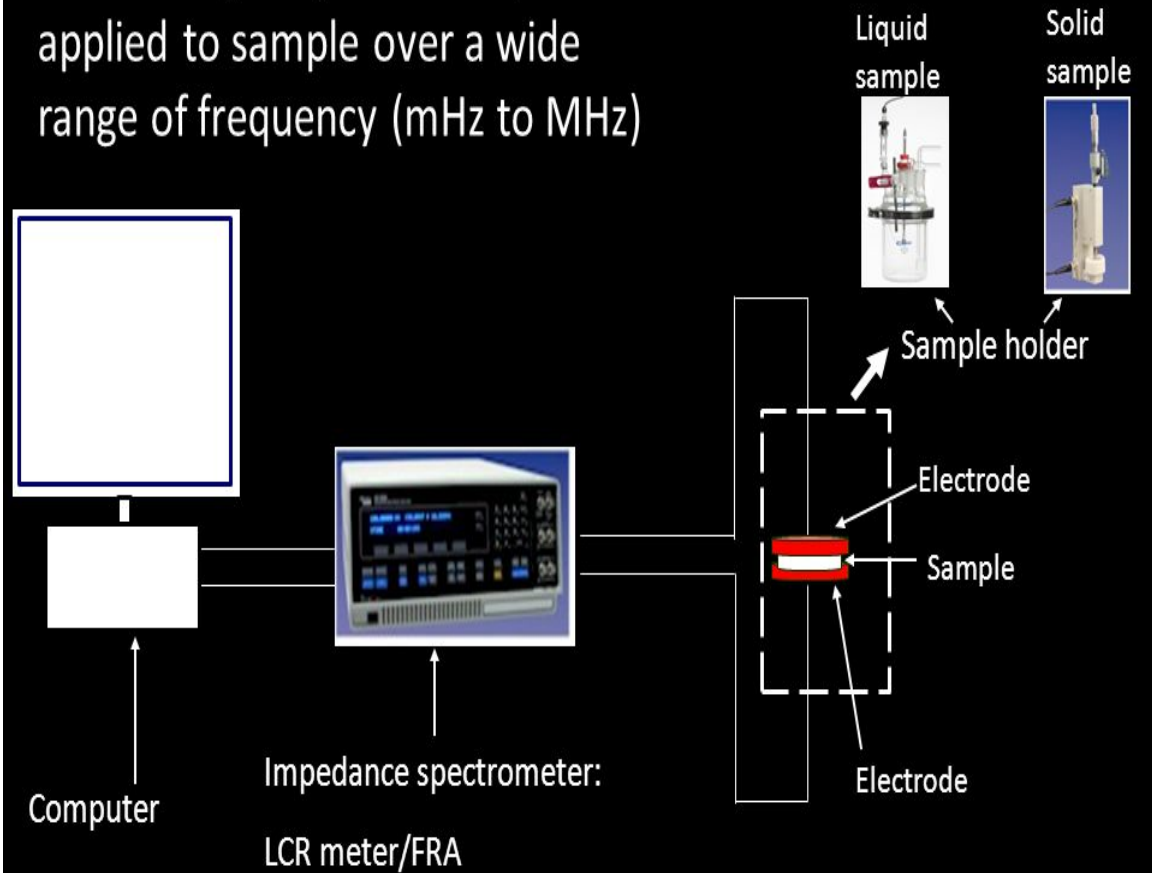
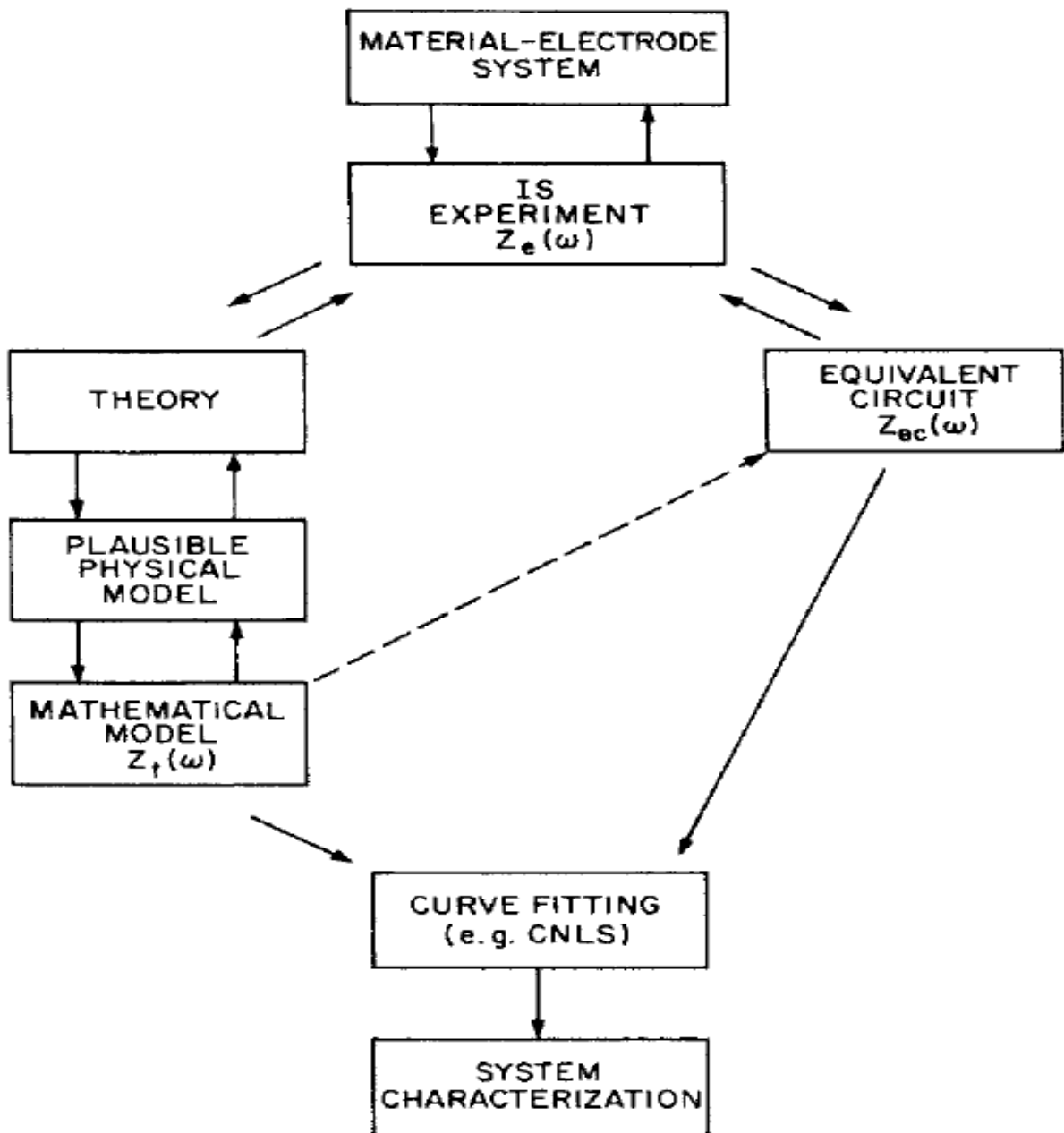


Fig 3. 7 Illustration of the setup for IS



Flow chart for the measurement and characterization of a material–electrode system

For analyzing the results of impedance technique, two types of plots are used mainly which are

- Nyquist Plot
- Bode Plot

**Nyquist Plot:**

In this type of plot x-axis of the plot shows the real part of impedance whereas y-axis represents its imaginary part. Each point on the nyquist plot gives the value of impedance at specific frequency with  $\arg Z$  as an angle between Vector  $Z$  and x-axis.

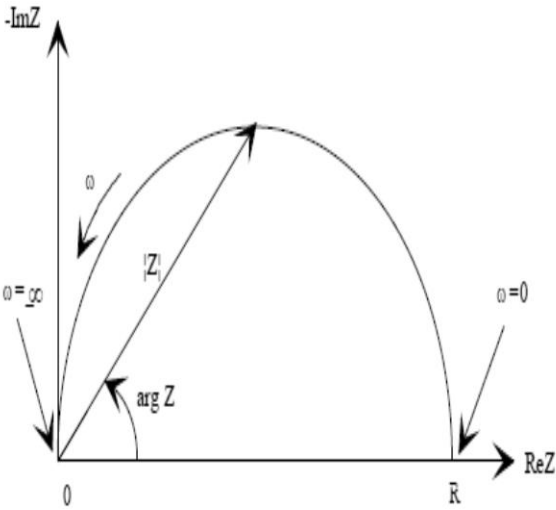


**Fig 3. 8 Nyquist Plot**

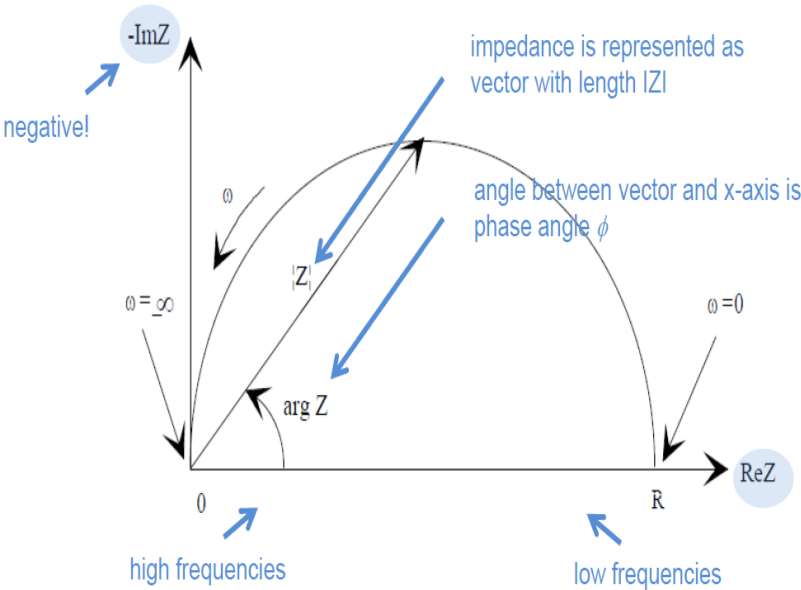


**Fig 3. 9 Nyquist plot as a function of frequency**

**Bode Plot:**

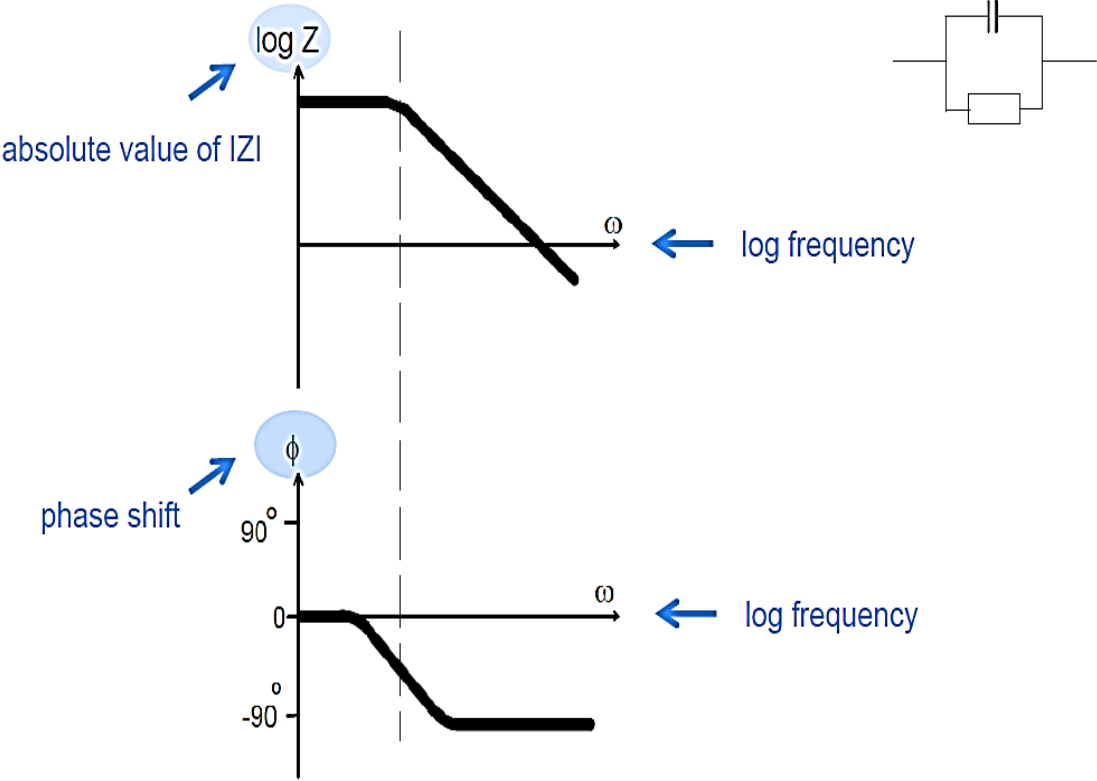


**Fig 3. 10 A typical Bode Plot**



## 3.3.2) Elementary Analysis Of Impedance Spectra

### 3.3.2.1) IS Plots of some model systems:

An elaborated physioelectrical model which possibly can occur for investigation of an electrode-material system might be unavailable or too complicated to be used in its initial form. For that, a very sophisticated approach is used in which the experimental impedance data  $Z_e(\omega)$  is approximated by the impedance of an equivalent circuit  $Z_{ec}(\omega)$  which comprised of set of ideal resistors, capacitors, probably inductors and other distributed circuit elements[48]. In these circuits a resistance represents a conductive path and for a given equivalent circuit the presence of resistor might points out towards the bulk conductivity of that reference material. Similarly, the presence of capacitors and inductors is associated with space charge polarization.

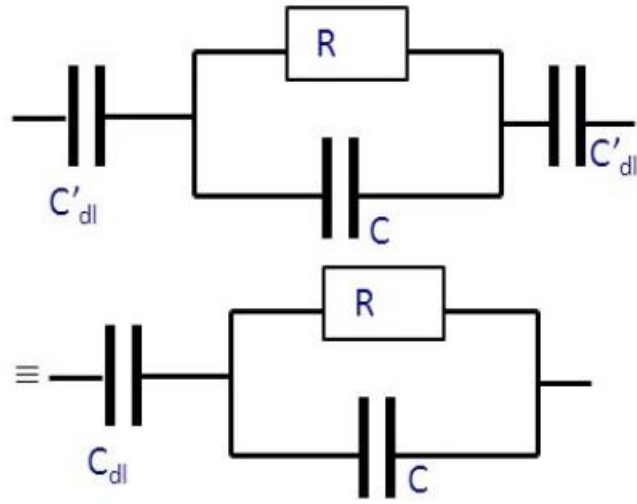
#### Ionic solid with two blocking electrodes:

In this particular example there are two double layer of charges at electrode/electrolyte interfaces and two double layer capacitances at the interfaces  $C'_{dl}$ .

In following Figures the equivalent circuit and expected impedance plots are shown.



Equivalent circuit



$C_{dl}$  = effective double layer capacitance

Fig3. 11 Equivalent circuit

Expected impedance plot

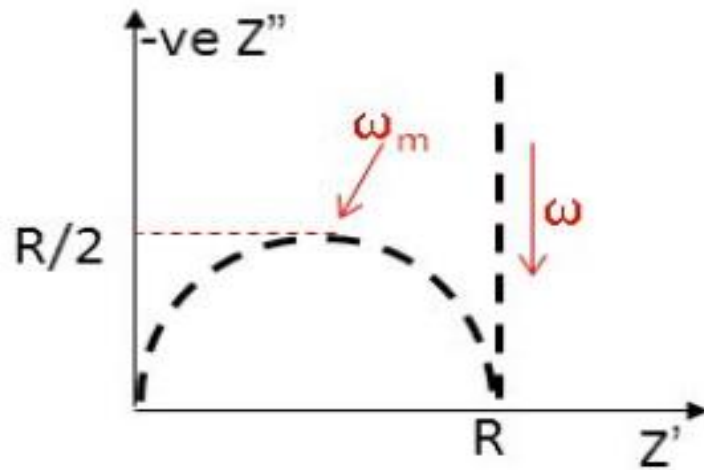
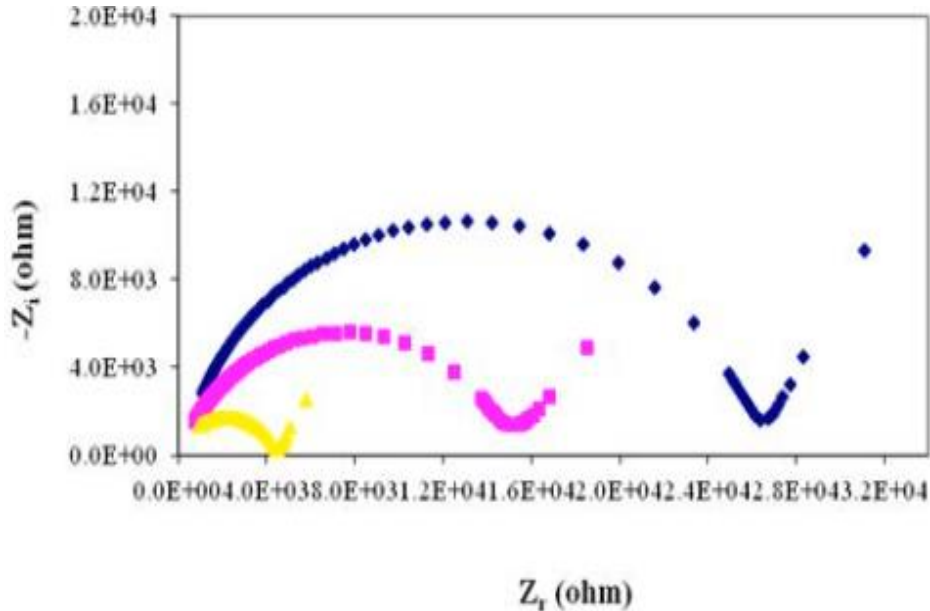


Fig3. 12 Impedance plot for the equivalent circuit

Following Figure represents the IS graph of experimental results of an ionic solid with two blocking electrodes



**Fig 3. 13 Experimental results of the given example[48]**

IS plots of real systems are a bit complicated. They deviate from ideal behavior. Distorted semicircles may arise due to overlap of semicircles with various time constants. Depressed semicircles arise if electrolyte is not homogenous i.e distributed microscopic properties of the electrolyte. Slanted spikes can also arise which are due to unevenness of electrode/electrolyte interfaces.

# Chapter 4: Results and discussions

---

## 4.1) X-Ray Diffraction:

XRD was carried out to investigate the effect of different doping concentration of Erbium and copper on the structural properties of Zinc Oxide (ZnO). Fig 4.1 shows XRD patterns of undoped and Er,Cu doped ZnO samples annealed at 450 °C. The peaks in the XRD patterns could be indexed as (100), (002), (101), (102), (110), (103), (200), (112) and (201) plane indicating a wurtzite hexagonal crystal structure. No doubtful peak was observed in the XRD pattern which eliminates the possibility of any secondary phase. XRD results presented here are in accordance with JCPDS card number **043-0002** suggesting that there is complete substitutional doping of Erbium and Copper into ZnO crystal lattice even upto 1% doping. In section 4.1.1 the crystallite size and associated microstrain for all the samples is calculated and is listed in table 4.1.

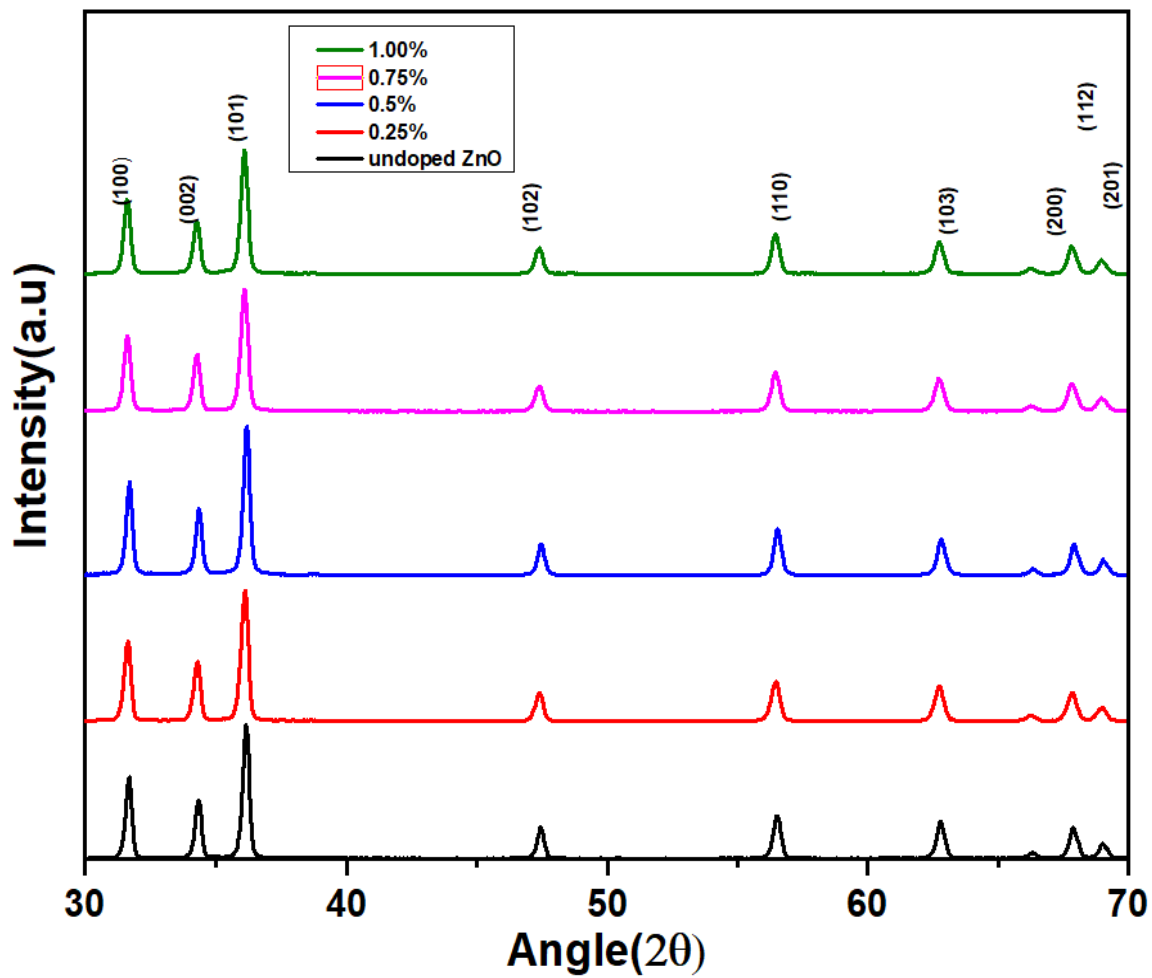


Fig4. 1 XRD pattern of un doped and co-doped samples of ZnO

### 4.1.1) Calculation of crystallite size and Micro Strain from XRD data using Williamson-Hall (W-H) Plot:

In XRD data, the broadening of the peaks is due to the combined effect of crystallite size ( $\beta_D$ ) and microstrain ( $\beta_\epsilon$ ), i.e

Total Broadening= Broadening due to crystallite size+ Broadening due to strain

$$\beta_T = \beta_D + \beta_\epsilon \quad \text{i)}$$

From Debye Scherrer equation we know that  $D = \frac{k\lambda}{\beta_D \cos\theta}$  so

$$\beta_D = \frac{k\lambda}{D \cos\theta} \quad \text{ii)}$$

where  $\beta_D$  is the Full width half maximum(FWHM) in radians i.e broadening of the peak.

k= "shape factor"

$\lambda$ = "0.15406nm is the wavelength of the X-ray source"

D= "crystallite size" and

$\theta$ = "peak position in radians"

The XRD peak broadening due to microstrain is given by

$$\beta_\epsilon = 4\epsilon \tan\theta \quad \text{iii)}$$

plugging ii) and iii) in eq i)

$$\beta_T = \frac{k\lambda}{D \cos\theta} + 4\epsilon \tan\theta$$

as we know that  $\tan\theta = \sin\theta / \cos\theta$ , so

$$\beta_T = \frac{k\lambda}{D \cos\theta} + \frac{4\epsilon \sin\theta}{\cos\theta}$$

multiplying  $\cos\theta$  on both sides results in

$$\beta_T \cos\theta = k\lambda/D + 4\epsilon\sin\theta$$

$$\beta_T \cos\theta = \epsilon(4\sin\theta) + \frac{k\lambda}{D}$$

This equation represents a straight line equation, in which  $\epsilon$  is the gradient(slope) of the line, and " $k\lambda/D$ " is the y-intercept.

Consider the standard equation of a straight line.

$$y = mx + c$$

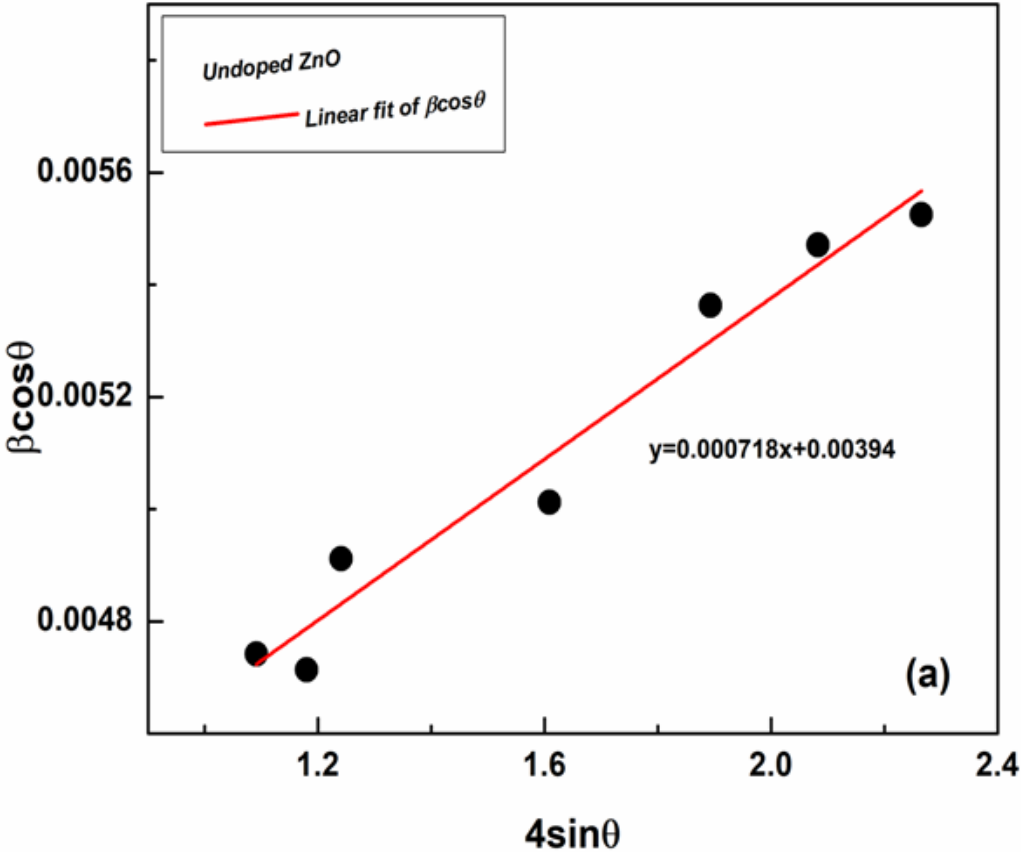
so we have;

$$y = \beta_T \cos\theta, \quad x = 4\sin\theta, \quad m = \epsilon \quad \& \quad c = \frac{k\lambda}{D}$$

So, " $4\sin\theta$ " will be plotted on x-axis and " $\beta_T \cos\theta$ " on the y-axis. Value of " $m$ " which represents the gradient of the line is the value of strain " $\epsilon$ ". Finally, the crystallite size will be calculated from y-intercept i.e. " $\frac{k\lambda}{D}$ ".

This rudimentary difference allows a separation of reflection broadening when both microstructural causes i.e. crystallite size and micro strain occur at the same time. The value of Microstrain( $\epsilon$ ) of all the samples is calculated from the slope( $m$ ) of fitted line i.e. least square fitting and particle size is calculated from the y-intercept of the fitted line. The equation of straight line of all the graphs has been shown. The Williamson-Hall plots show that line broadening is isotropic and there is essentially a contribution of microstrain present here. The value of Microstrain and particle size for undoped and co-doped ZnO samples is listed in the table below;

The value of microstrain( $\epsilon$ ) and particle size(nm) is listed in the table 4.1 calculated from Williamson Hall(W-H) method. It is clearly seen that particle size of undoped sample of ZnO is larger than other samples while 0.75% Er,Cu doped sample has lowest strain and comparatively larger particle size than 0.25,0.5 and 1% co-doped samples. The particle size of undoped sample is 36.755nm which starts to decrease when doped with different concentrations of Erbium and copper, depicting the successful doping of Erbium and copper at Zinc sites.





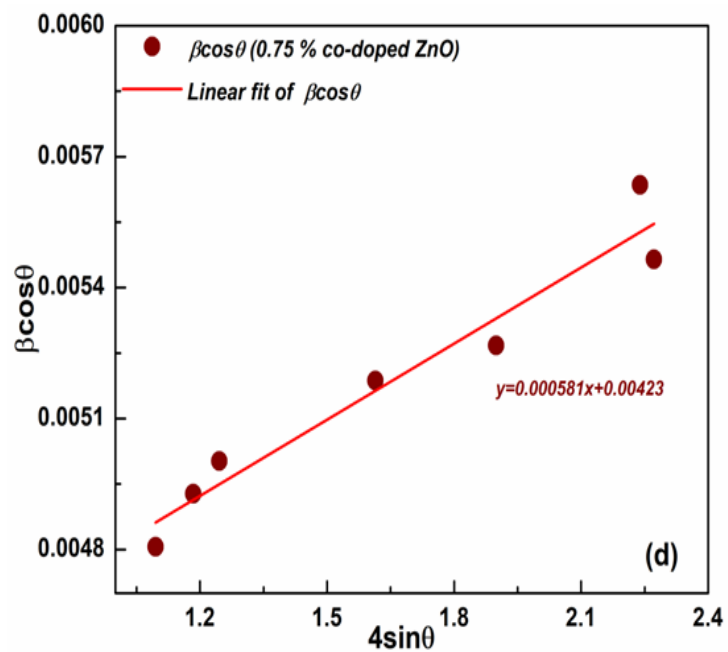
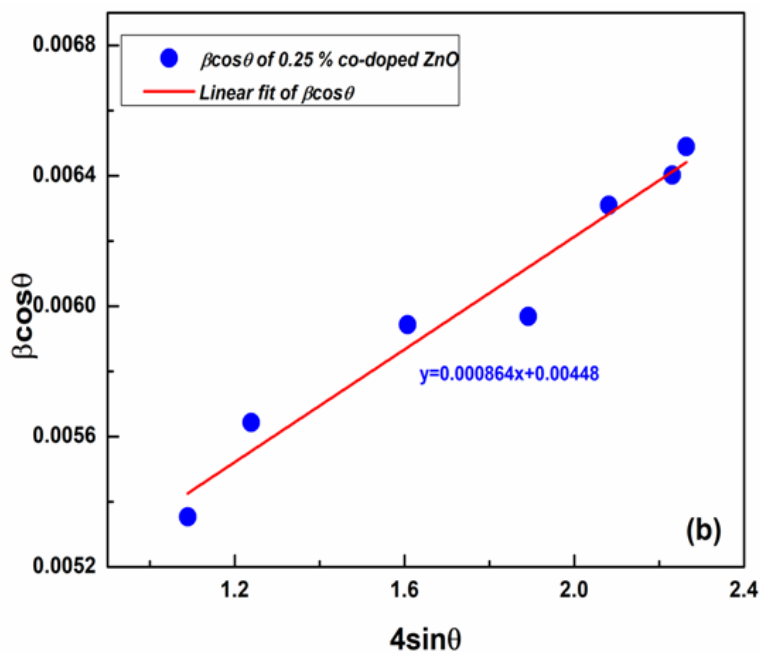


Fig 4. 2 W-H Plot of un-doped ZnO

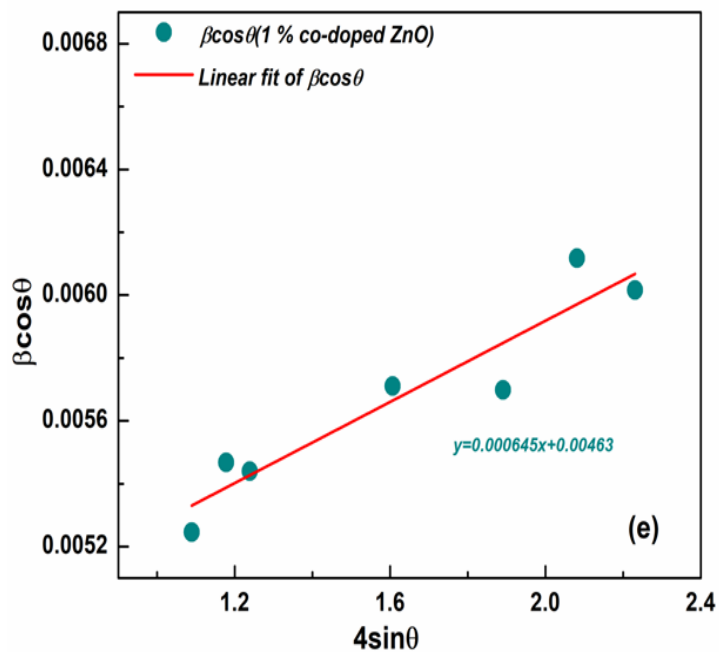
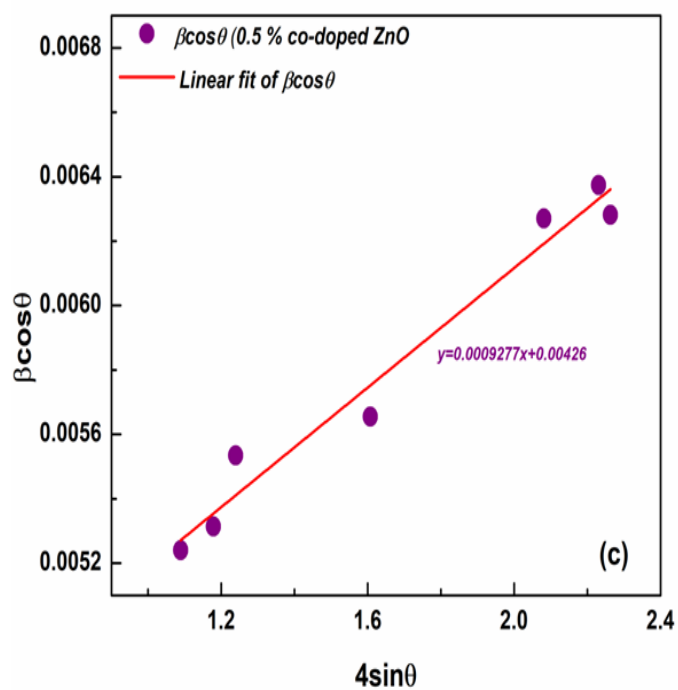


Fig 4. 3 W-H Plots of 0.25, 0.5, 0.75 and 1% co-doped ZnO

The value of Microstrain and particle size for undoped and co-doped ZnO samples is listed in the table below;

<b>Doping %age</b>	<b>Micro strain(<math>\epsilon</math>)</b>	<b>Particle size(D)nm</b>	<b>Estimated error in microstrain <math>\pm</math></b>
Un-doped ZnO	0.000718	36.755	0.000062
0.25% co-doped ZnO	0.000864	32.325	0.000080
0.5% co-doped ZnO	0.000927	33.994	0.000072
0.75% co-doped ZnO	0.000581	34.235	0.000062
1.00% co-doped ZnO	0.000645	31.277	0.000098

**Table 4.1: Microstrains and particle size of all samples**

#### 4.2) Band Gap Calculation using Kubelka-Munk Treatment:

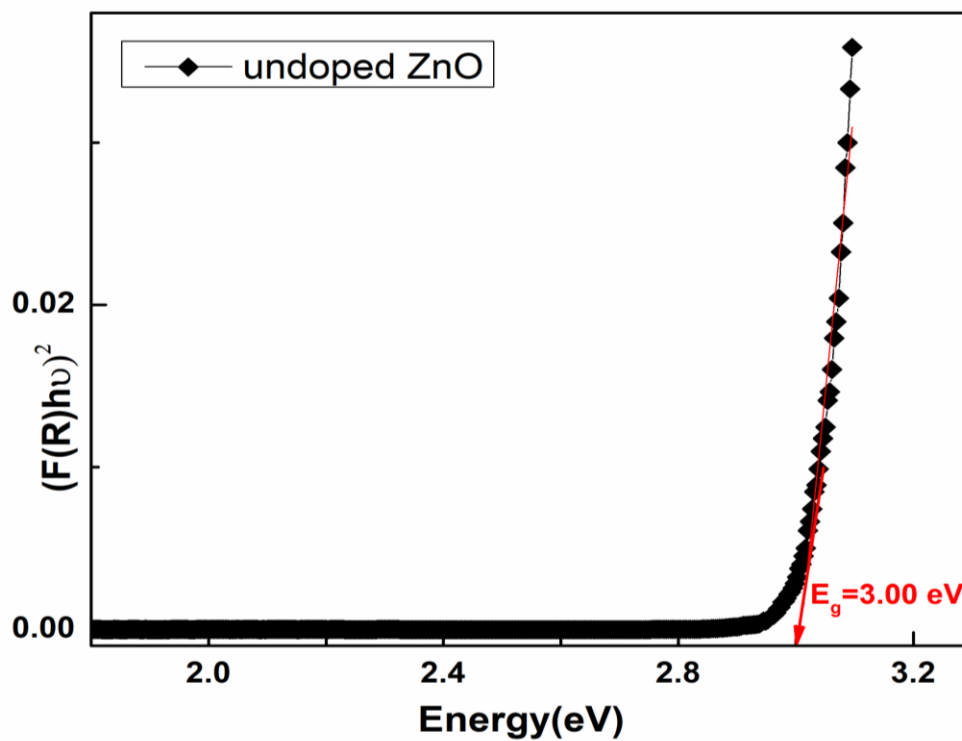


Fig 4. 4 Diffuse Reflectance spectra (Band Gap energies) i.e Munk plot of undoped ZnO

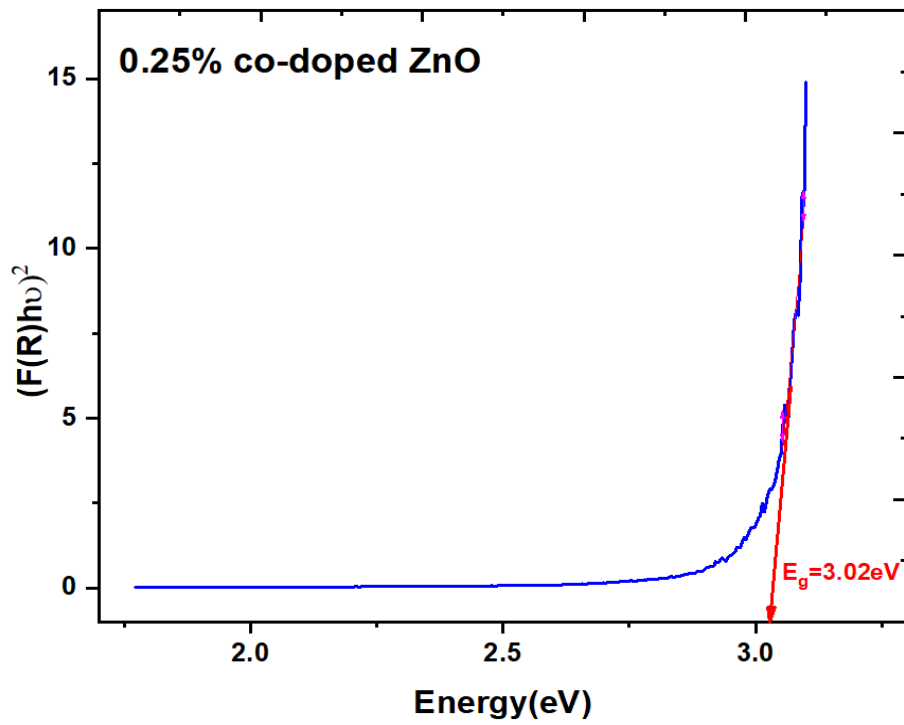


Fig 4. 5 Munk plot of 0.25% Er,Cu doped ZnO

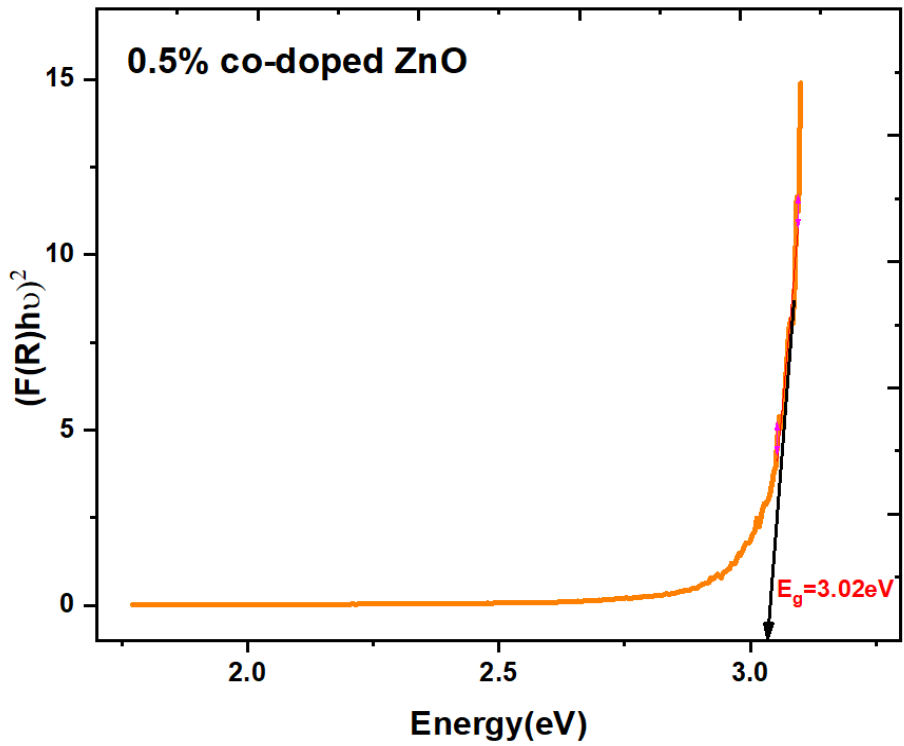
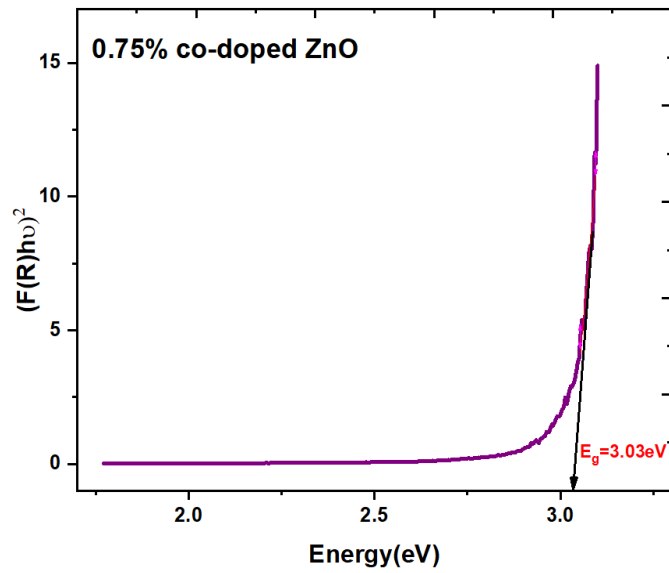
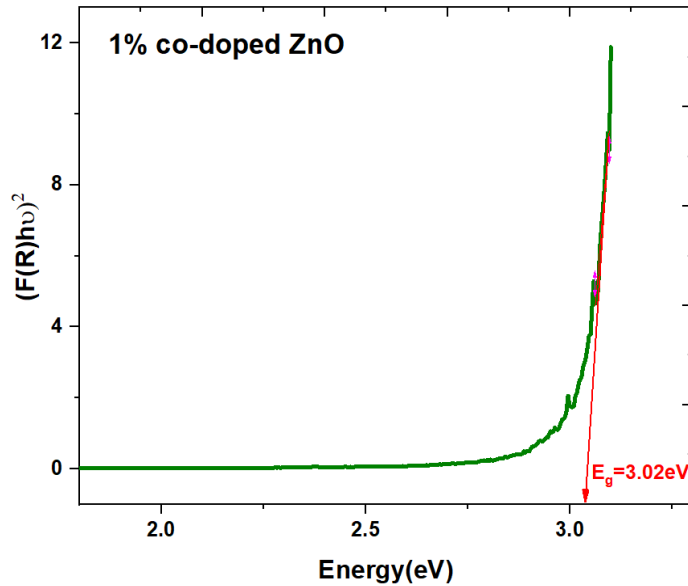


Fig 4. 6 Munk plot of 0.5% Er,Cu doped ZnO



**Fig4. 7 Munk plot of 0.75% Er,Cu doped ZnO**



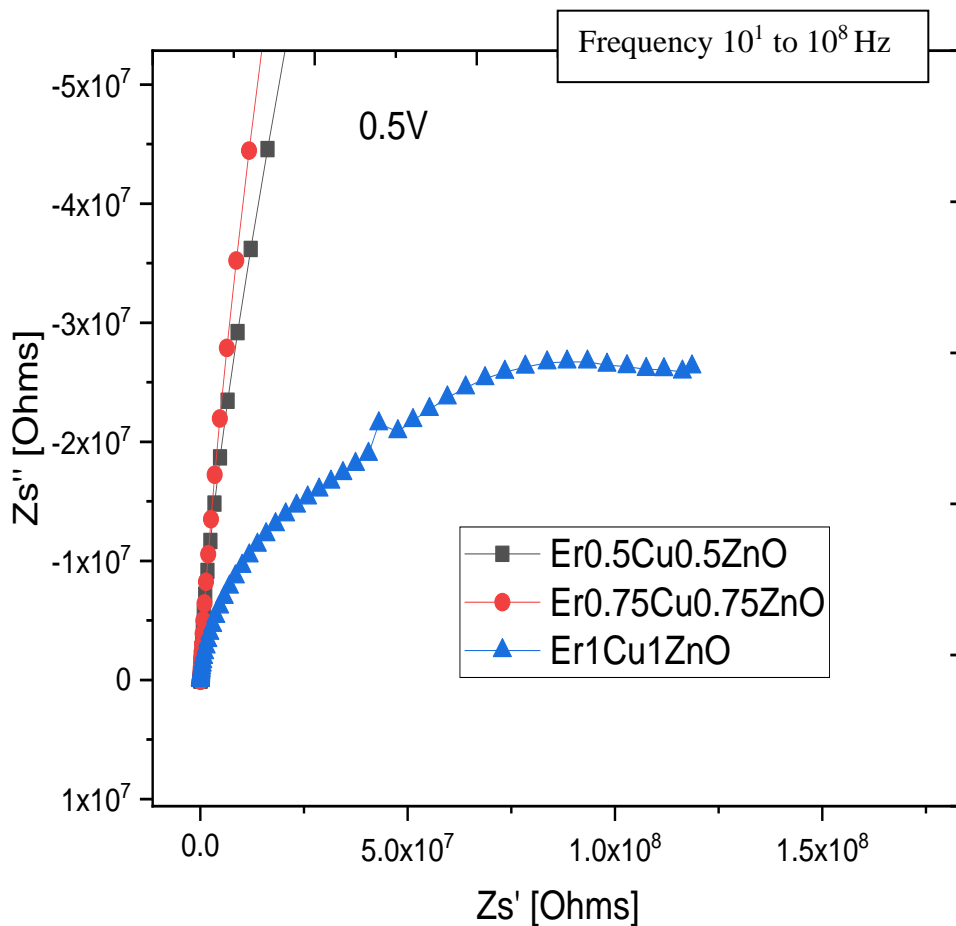
**Fig4. 8 Munk plot of 1% Er,Cu doped ZnO**

- Band gaps of co-doped samples are determined using Kubelka-Munk treatment and they come out to be 3.00, 3.02, 3.02, 3.03, and 3.02eV for pure, 0.25,0.5, 0.75 and 1% Er, Cu doped ZnO samples respectively.
- There is no visible change in the bandgap with increasing doping concentration.

## 4.3) Impedance Analysis:

### 4.3.1) Impedance plan plot ( $Z'$ Vs $Z''$ ):

For 0.5, 0.75 and 1% co-doped ZnO samples impedance plan plots as a parametric function of frequency are shown in Fig and Fig. The experimental data is represented by solid symbols and the joining lines are just guidelines to the eyes as shown in Figures. In case of purely resistive or capacitive behavior the plan plots curvatures appear to be in the form of straight lines along real and imaginary axis of impedance ( $Z$ ). But when, there is capacitive and resistive behavior at the same time then the response is the semicircle.



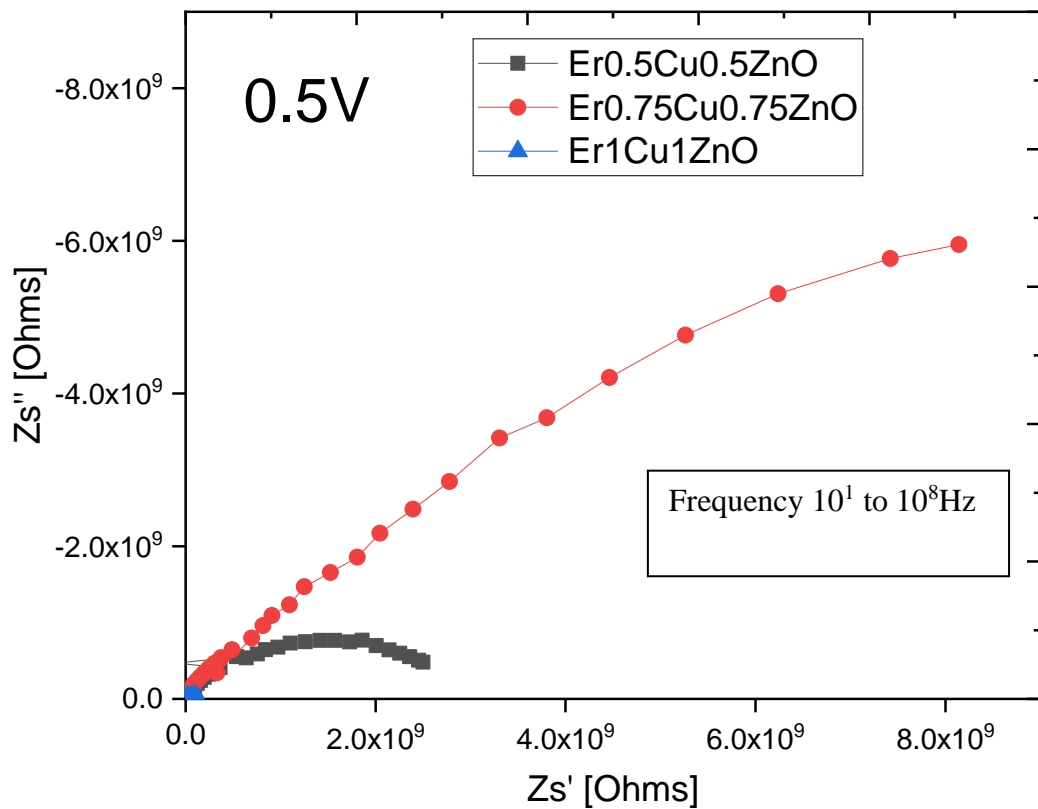


**Fig4. 9 Nyquist plots of 0.5 0.75 and 1% co-doped ZnO**

Generally the size of the semicircle in high frequency region determines the resistance in charge transfer between the electrode surface and interface. The diameter of a semicircle determines the charge transfer resistance.

Grain boundaries are more resistive than grains in ceramics, possible reason for that could be the presence of oxygen and existence of dangling bonds at grain boundaries. The increased capacitance and resistance is related to grain boundaries associated to low frequency range as compared to grains. In polycrystalline materials the ac signal relates the affect of electrode, semiconductor contact, inter and intra grain boundaries at different frequency range. [59] The ZnO system along with varied amount of dopants comprise of micro-structural heterogeneities like grain, grain boundaries or porosity etc. If an element is present with larger RC product it suggests that mobility of charge carries is low across that element which can result into a higher value of dielectric constant. The resistance of including micro-structure elements are represented by the diameter of a semicircular arc given on  $Z'$ -axis, while the total resistance of all the heterogeneities present in the system is sum of all diameters of appearing arcs in impedance plots [59]. In ZnO and other metal

oxides, the resistance of grains is less as compare to grain boundaries so the arc which represents the grain boundaries contributions lies on less frequency region for this reason the grain boundaries have much larger relaxation time as compare to the grain due to presence of point defects (i.e. Oxygen vacancies, Zinc interstitial & Zn vacancies etc.) at grain boundaries [59].

#### 4.3.2) Frequency Vs Dielectric Constant:

As we know that dielectric spectroscopy study gives us a good insight about grain, grain boundaries, charge transport and charge storage properties of a dielectric material. Dielectric properties of a material depend upon several factors including its chemical composition as well as method of preparation.

The frequency dependence of the real part of permittivity of 0.5, 0.75 and 1% Er, Cu doped ZnO is shown below. The dielectric response for all the samples clearly reveal a dispersion region in the high frequency range ( $>10^4$  Hz). Dispersion region also known as plateau region for dielectric constant is the area where value of  $\epsilon'$  stays unaffected. Generally the dipoles follow the applied ac field at less frequency range i.e ( $f < f_r = 1/2\pi\tau_r$ ) where  $f_r = 1/2\pi\tau_r$  is the relaxation frequency. But as the frequency increases dipoles lag behind the field and  $\epsilon'$  decreases. When frequency approaches to a certain value i.e relaxation frequency  $f_r = 1/2\pi\tau_r$ , dipoles don't follow the field causing a sudden decline in real part of dielectric constant.

- The dielectric dispersion can be explained by the dominance of grain boundaries effect, it is a general trend in metal oxides that with an increase in frequency the real part of the dielectric constant decreases. This is attributed to **Maxwell–Wagner** type of interfacial polarization in accordance with Koop's theory [60, 61].
- It can be seen from the results that 1% co-doped sample has a highest value of dielectric constant and that serves the purpose of doping i.e by increasing the amount of doping dielectric constant of ZnO increases.



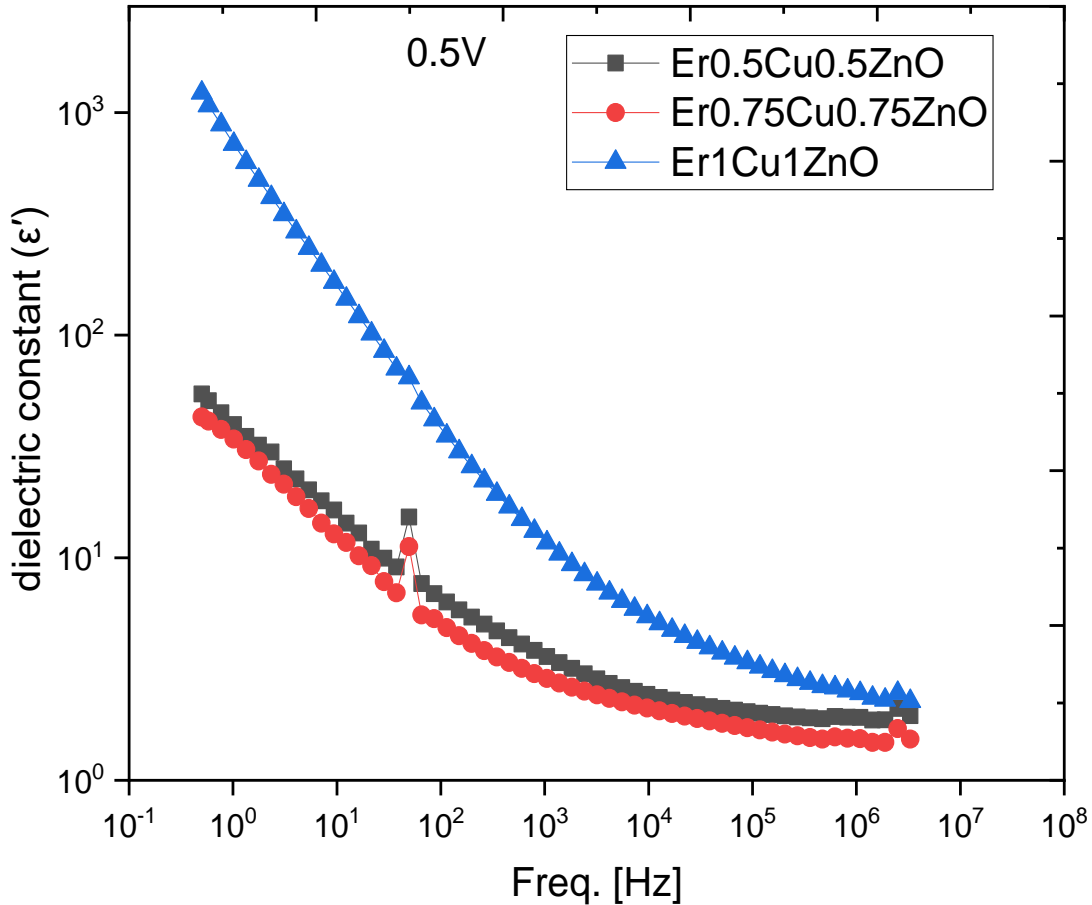


**Fig 4. 10** Variation of real part of the dielectric constant w.r.t frequency for 0.5, 0.75 and 1% co-doped ZnO annealed.

#### 4.3.3) Frequency Vs Tangent losses:

- Tangent loss determines the energy loss of a system. It is the ratio of imaginary part to the real part which tells us about the amount of energy lost to the amount of energy stored in a material. Basically it is attributed to the imperfections and impurities present in a material resulting in a decrease in the value of polarization. It can be observed from the following graph that dielectric loss in the represented samples decreases with an increase in frequency. It is higher at lower frequencies and gradually decreases with increasing frequency.
- This behavior can be explained by the phenomenological Koop's Theory [60] that tells us that the effect of grain boundaries and amount of associated resistivity is

higher at low frequencies resulting in higher loss of energy as it requires more energy for the exchange of electrons there. In contrary to that at higher frequencies there is low value of resistivity due to dominance of grains over grain boundaries.

- It can be seen from the graph below that for the 1% co-doped sample the value of dielectric loss is highest. It can be put in this way that as in section 4.3.2 we have seen that this particular sample has the highest value for the dielectric constant i.e the effect of resistivity due to grain boundaries is maximum, hence it requires more energy for the electrons to conduct resulting in more losses and higher dielectric constant.

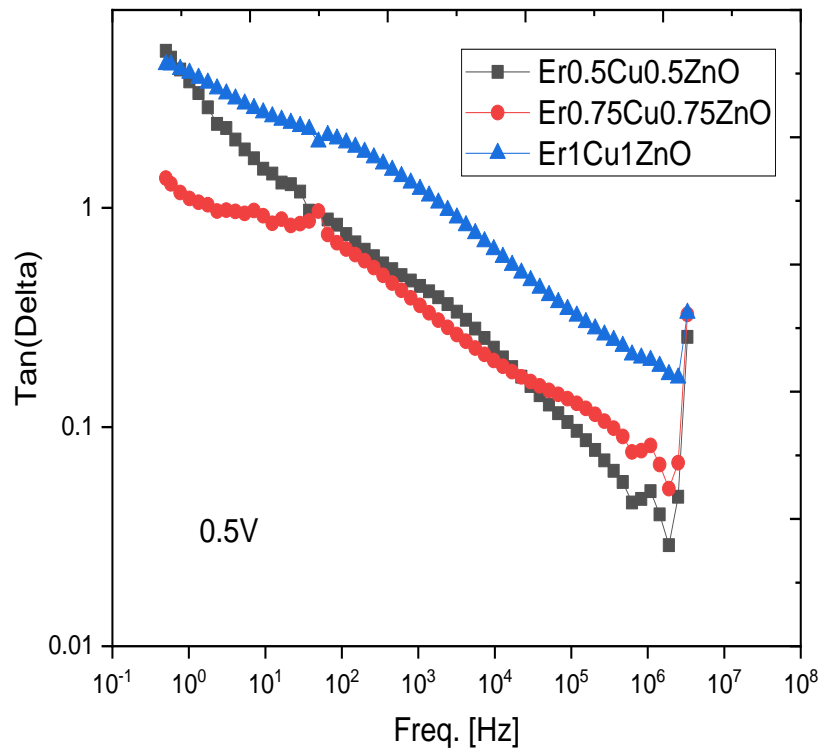


**Fig 4. 11** Variation of tangent loss w.r.t frequency for 0.5,0.75 and 1% co-doped ZnO

## Future Recommendations:

- Oxides of both dopants (donor(Erbium) and acceptor (copper) have good dielectric properties. Nano-composite of these oxides with ZnO might introduce interface effects that can open up a new dimension for the realization of huge permittivity in ZnO with very low dielectric losses.
- This approach will extend horizon for the search of frequency and temperature independent CP in ZnO which will be of great importance for the miniaturization of current electronic industry.

## Conclusion:

- From XRD results it has been proved that both Erbium and copper are successfully doped in ZnO with 0.25, 0.5, 0.75 and 1%M doping concentrations.
- Band gap analysis of all the samples is done using UV visible Diffuse Reflectance Spectroscopy, and we observed no visible change in the bandgaps of samples.
- Impedance analysis of the samples confirmed the colossal permittivity in ZnO which increases with an increase in doping concentration. 1% co-doped ZnO sample has a maximum value of dielectric constant.
- The value of real part of dielectric constant and tangent loss decreases with an increase in frequency while ac conductivity increases with an increase in frequency.

# Bibliography:

- [1] Hernandezbattez, A; Gonzalez, R.; Viesca, J.; Fernandez, J.; Diazfernandez, J.; MacHado, A.; Chou, R.; Riba, J. (2008). "CuO, ZrO<sub>2</sub> and ZnO nanoparticles as antiwear additive in oil lubricants". *Wear*. 265 (3–4): 422–428.
- [2] Porter, F. (1991). *Zinc Handbook: Properties, Processing, and Use in Design*. CRC Press.
- [3] Dal Corso, Andrea; Posternak, Michel; Resta, Raffaele; Baldereschi, Alfonso (1994). "Ab initio study of spontaneous polarization in ZnO". *Physical Review B*. 50(15):10715
- [4] Özgür, Ü.; Alivov, Ya. I.; Liu, C.; Teke, A.; Reshchikov, M. A.; Doğan, S.; Avrutin, V.; Cho, S.-J.; Morkoç, H. (2005). "[A comprehensive review of ZnO materials and devices](#)".
- [5] Look, D.C.; Hemsley, J.W.; Sizelove, J.R. (1999). "Residual Native Shallow Donor in ZnO". *Physical Review Letters*.
- [6] Janotti, A. & Van De Walle, C.G. (2007). "Hydrogen multicentre bonds". *Nature Materials*.
- [7] Kato, H; Sano, Michihiro; Miyamoto, Kazuhiro; Yao, Takafumi (2002). "Growth and characterization of Ga-doped ZnO layers on a-plane sapphire substrates grown by molecular beam epitaxy". *Journal of Crystal Growth*.
- [8] Nunes P, Fernandes B, Fortunato E, Vilarinho P, Martins R (1999). Performance presented by ZnO thin films deposited by spray pyrolysis. *Thin Solid Films*, 337: 176
- [9] Chopra L, Major S, Pandya D K, Restage R S, Vankar VD (1983). Thermal device applications. *Thin Solid Films*, 1021: 1-4
- [10] Kim H, Gilmore CM (2000). Transparent conducting aluminum -doped zinc oxide thin films for organic light emitting devices. *Appl. Phys. Lett.*, 76: 259
- [11] Chopra L, Major S, Pandya D K, Restage R S, Vankar VD (1983). Thermal device applications. *Thin Solid Films*, 1021: 1-4
- [12] ] Zhang DH , Xue ZY, Wang QP (2002). The mechanism of blue emission from ZnO films deposited on glass substrate by r.f magnetron sputtering. *J. Phys. D Appl. Phys.*, 35: 2837- 2841.

- [13] Moezzi, Amir; McDonagh, Andrew M.; Cortie, Michael B. (2012). "Review: Zinc oxide particles: Synthesis, properties and applications". *Chemical Engineering Journal*. 185–186:
- [14] Van Noort, Richard (2002). *Introduction to Dental Materials*(2d ed.). Elsevier Health Sciences.
- [15] Harding, Fred John (2007). *Breast Cancer: Cause – Prevention – Cure*. Tekline Publishing. p. 83.
- [16] British National Formulary (2008). "Section 13.2.2 Barrier Preparations".
- [17] "Critical Wavelength & Broad Spectrum UV Protection". mycpss.com. Retrieved 15 April 2018.
- [18] Nav Bharat Metallic Oxide Industries Pvt. Limited. Applications of ZnO. Archived February 26, 2009, at the Wayback Machine Access date January 25, 2009
- [19] ] Klingshirn, C. (2007). "ZnO: Material, Physics and Applications". *ChemPhysChem*. 8 (6): 782–803.
- [20] Guedri-Knani, L; et al. (2004). "Photoprotection of poly(ethylene-naphthalate) by zinc oxide coating". *Surface and Coatings Technology*. 180–181: 71–75.
- [21] Nakamura S and Chichibu S F (ed) 2000 Nitride Semiconductor Blue Lasers and Light Emitting Diodes(Boca Raton, FL: CRC Press)
- [22] M. Buscaglia, M. Viviani, V. Vuscaglia, L. Mitoseriu, A. Testino, P. Nanni, Z. Zhao, M. Nygren, C. Harnagea, D. Piazza, C. Galassi, *Phys. Rev. B* 73 (2006)
- [23] J. Wu, C.-W. Nan, Y. Lin, Y. Deng, *Phys Rev. Lett.* 89 (2002)
- [24] M. A. Subramanian, D. Li, N. Duan, B. A. Reisner, A. W. Sleight, *J. Solid State Chem.*, 151 (2000) 323
- [25] W. Hu, Y. Liu, R. L. Withers, T. J. Frankcombe, L. Noren, A. Snashall, M. Kitchin, P. Smith, B. Gong, H. Chen, J. Schiemer, F. Brink, J. Wong-Leung, *Nat. Mater.*, 12 (2013) 821
- [26] S. Sarkar, P. K. Jana, B. K. Chaudhuri, *Appl. Phys. Lett.*, 92 (2008) 022905
- [27] S. Krohns, P. Lunkenheimer, S. Meissner, A. Reller, B. Gleich, A. Rathgeber, T. Gaugler, H. U. Buhl, D. C. Sinclair, A. Loidl, *Nat. Mater.* 10, 899 (2011)
- [28] J. Dumas, C. SCHLENKER, J. Marcus, R. Buder, *Phys. Rev. Lett.* 50, 757 (1983)

- [29] C. J. Raj, G. Paramesh, B. S. Prakash, K. R. S. P. Meher, K. B. R. Varma, Mater. Res. Bull., 74 (2016)
- [30] Fundamentals of zinc oxide as a semiconductor Anderson Janotti and Chris G Van de Walle
- [31] Zhang S B, Wei S-H and Zunger A 2001 Phys. Rev. B 63 075205
- [32] Janotti A and Van de Walle C G 2006 J. Cryst. Growth 287 58
- [33] Erhart P and Albe K 2006 Phys. Rev. B 70 115207
- [34] Lany S and Zunger A 2005 Lany S and Zunger A 2007 Phys. Rev. Phys. Rev. B 72 035215 Lett. 98 045501
- [35] Patterson C H 2006 Phys. Rev. Lett. 74 144432
- [36] Janotti A and Van de Walle C G 2007 Phys. Rev. B 6 44
- [37] Janotti A and Van deWalle C G 2007 Phys. Rev. B 75 165202
- [38] Cox S F J et al 2001 Phys. Rev. Lett. 86 2601
- [39] Hofmann D M, Hofstaetter A, Leiter F, Zhou H, Henecker F, Meyer B K, Orlinskii S B, Schmidt J and Baranov P G 2002 Phys. Rev. Lett. 88 045504
- [40] McCluskey M D, Jokela S J, Zhuravlev K K, Simpson P J and Lynn K G 2002 Appl. Phys. Lett. 81 3807
- [41] Charles Kittel, "Introduction to Solid State Physics", John Wiley and Sons Inc.:Newyork (1976)
- [42] <http://www.microscopy.ethz.ch/bragg.htm>
- [43] Scott M. Juds (1988). Photoelectric sensors and controls: selection and application. CRC Press. p. 29. ISBN 978-0-8247-7886-6. Archived from the original on 2018-01-14.
- [44] P. Kubelka and F. Munk, Z. Tech. Phys. 12 (1931) 593
- [45] J. Torrent and V. Barrón, Encyclopedia of Surface and Colloid Science. (Marcel Dekker, Inc.: New York, 2002).
- [46] R.A. Smith, *Semiconductors*, 2nd ed. (Cambridge University Press: Cambridge, 1978).
- [47] CS Nichols, CG Van de Walle, and ST Pantelides, "Mechanisms of equilibrium and nonequilibrium diffusion of dopants in silicon", Physical review letters, **62**(9), (1989) 1049.

- [48] E Barsoukov, and J R Macdonald, "Impedance spectroscopy: theory, experiment, and applications", John Wiley & Sons (2018).  
M. Buscaglia, M. Viviani, V. Buscaglia, L. Mitoseriu, A. Testino, P. Nanni, Z. Zhao,
- [49] M. Nygren, C. Harnagea, D. Piazza, C. Galassi, High dielectric constant and frozen macroscopic polarization in dense nanocrystalline BaTiO<sub>3</sub> ceramics, *Phys. Rev. B* 73 (2006).
- [50] M.A. Subramanian, D. Li, N. Duan, B.A. Reisner, A.W. Sleight, High dielectric constant in ACu<sub>3</sub>Ti<sub>4</sub>O<sub>12</sub> and ACu<sub>3</sub>Ti<sub>3</sub>FeO<sub>12</sub> phases, *J. Solid State Chem.* 151 (2000) 323e325.
- [51] J. Wu, C.-W. Nan, Y. Lin, Y. Deng, Giant dielectric permittivity observed in Li and Ti doped NiO, *Phys. Rev. Lett.* 89 (2002).
- [52] S. Sarkar, P.K. Jana, B.K. Chaudhuri, Colossal internal barrier layer capacitance effect in polycrystalline copper (II) oxide, *Appl. Phys. Lett.* 92 (2008) 022905.
- [53] W. Hu, Y. Liu, R.L. Withers, T.J. Frankcombe, L. Nor\_en, A. Snashall, M. Kitchin, P. Smith, B. Gong, H. Chen, J. Schiemer, F. Brink, J. Wong-Leung, Electronpinned defect-dipoles for high-performance colossal permittivity materials, *Nat. Mater.* 12 (2013) 821e826.
- [54] C.J. Raj, G. Paramesh, B.S. Prakash, K.R.S.P. Meher, K.B.R. Varma, Origin of giant dielectric constant and conductivity behavior in Zn<sub>1-x</sub>Mg<sub>x</sub>O (0 < x < 0.1) ceramics, *Mater. Res. Bull.* 74 (2016) 1e8.
- [55] Colossal permittivity and dielectric relaxation of (Li, In) Co-doped ZnO Ceramics  
Dong Huang Zhifu, Liu Yongxiang Li. Yun Liu
- [56] Hu J and Gordon R G 1992 *J. Appl. Phys.* **71** 880

[57] Hu J and Gordon R G 1993 Mater. Res. Soc. Symp. Proc. 283891

[58] Block D, Hervé A and Cox R T 1982 *Phys. Rev. B* [25 6049](#)

[59] E Barsoukov, and J R Macdonald, “Impedance spectroscopy: theory, experiment, and applications”, John Wiley & Sons (2018).

[60] C. G. Koops *Phys. Rev.*, 1951, **83** , 121

[61] L. Chauhan , A. K. Shukla and K. Sreenivas , Dielectric and magnetic properties of Nickel ferrite ceramics using crystalline powders derived from DL alanine fuel in sol–gel auto-combustion, *Ceram. Int.*, 2015, **41** , 8341 —8351